A THESIS FOR THE DEGREE OF MASTER SCIENCE

Catalytic effects of potassium and magnesium on fast pyrolysis of yellow poplar and characteristics of pyrolytic products

칼륨과 마그네슘이 백합나무의 급속 열분해 공정 및 열분해 산물의 물리·화학적 특성에 미치는 영향 분석

by Hyewon Hwang

PROGRAM IN ENVIRONMENTAL MATERIALS SCIENCE
GRADUATE SCHOOL
SEOUL NATIONAL UNIVERSITY
FEBRUARY, 2014

A THESIS FOR THE DEGREE OF MASTER SCIENCE

Catalytic effects of potassium and magnesium on fast pyrolysis of yellow poplar and characteristics of pyrolytic products

칼륨과 마그네슘이 백합나무의 급속 열분해 공정 및 열분해 산물의
물리·화학적 특성에 미치는 영향 분석

by Hyewon Hwang

Advisor: Joon Weon Choi

PROGRAM IN ENVIRONMENTAL MATERIALS SCIENCE
GRADUATE SCHOOL
SEOUL NATIONAL UNIVERSITY
FEBRUARY, 2014

Catalytic effects of potassium and magnesium on fast pyrolysis of yellow poplar and characteristics of pyrolytic products

칼륨과 마그네슘이 백합나무의 급속 열분해 공정 및 열분해 산물의 물리·화학적 특성에 미치는 영향 분석

지도교수 : 최 준 원

이 논문을 농학석사학위논문으로 제출함

2013년 11월

서울대학교 대학원
산림과학부 환경재료과학 전공
황 혜 원

황혜원의 석사학위논문을 인준함

2013년 12월

위 원 장 _____ (인)

부위원장 _____ (인)

위 원 _____ (인)

Abstract

Catalytic effects of potassium and magnesium on fast pyrolysis of yellow poplar and characteristics of pyrolytic products

Hyewon Hwang
Program in Environmental Material Science
Graduate School
Seoul National University

The goal of this study was to investigate the catalytic effects of inorganic metals, especially potassium and magnesium, on the pyrolysis of lignocellulosics and the physicochemical properties of the corresponding products. In this study, thermogravimetric analysis (TGA) and fast pyrolysis were performed with demineralized and inorganic metal-impregnated yellow poplar wood. The fast pyrolysis was carried out at 450°C, 500°C, and 550°C with a residence time of 1.3 s. TGA results suggested that the maximum decomposition temperature of the biomass was more influenced by magnesium than potassium as it decreased from 373.9°C for demineralized biomass (D-YP) to 359.0°C for biomass with 2.0 wt% of potassium-impregnation (K-2.0) and to 337.6°C for biomass with 2.0 wt% of magnesium-impregnation (Mg-2.0). During the fast pyrolysis, the char yield was greatly influenced by inorganic metals, especially potassium. The char yield of potassium-impregnated biomass was doubled regardless of the pyrolysis temperature as compared to demineralized yellow poplar. The presence of potassium and magnesium also affected the properties of the bio-oil. With increasing potassium concentrations, the water content increased from 14.4 wt% to 19.7 wt% and the viscosity decreased from 34 cSt to 16 cSt, while the pH of the bio-oil remained stable. Magnesium induced a dehydration reaction leading to an increase in the water content, while the viscosity

increased from 45 cSt to 216 cSt and the pH decreased. Gas chromatography-mass spectroscopy (GC-MS) analysis revealed that potassium promoted thermochemical reactions, thus causing a decrease in the amount of levoglucosan and an increase in that of small molecules and lignin-derived phenols in the bio-oil. Magnesium, however, acted as a catalyst for the recombination reaction of levoglucosan and other small molecules to form large fractions such as oligomers and char particles in the bio-oil. Following the pyrolysis, most of the inorganic metals were distributed in the bio-char and the remaining amount depended on the temperature of the reaction. Additionally, various forms of aromatic hydrocarbons, probably derived from lignins, were detected in the non-condensed pyrolytic gas fractions.

Key words: fast pyrolysis, bio-oil, potassium, magnesium, char formation, inorganic distribution.

Student number: 2012-21122

Contents

List of Tables

List of Figures

1. Introduction

1.1. Fast pyrolysis of lignocellulosic biomass

Lignocellulosic biomass is considered a renewable and environment-friendly energy source, which cancontribute to the reduction of carbon dioxide emissions. It can be utilized as electricity, heat, bio-fuel, and chemical material via thermochemical processes such as pyrolysis, gasification, and combustion. Among those processes, fast pyrolysis has been deemed as one of the most promising methods to obtain liquid fuel, also referred to as “bio-oil” (Mohan et al., 2006).

Fast pyrolysis is the thermal decomposition that occurs in the absence of oxygen, in which biomass is rapidly heated at around 500°C with short vapor residence times (typically less than 2 s; Bridgwater et al., 1999). During the fast pyrolysis, the polymeric constituents of biomass are thermally degraded into numerous small molecules and are converted to volatile vapors that condense to form bio-oil. The main pyrolytic product, bio-oil, is a dark brown liquid composed of oxygenated hydrocarbons and char, solid separated by a cyclone. Non-condensable gasses are also produced from fast pyrolysis.

In general, the yield and physicochemical properties of bio-oil are closely related to the fields of the industrial application. They are affected by various factors including the chemical composition and size of the material and the process conditions, i.e., heating rate, process temperature, residence time, ambient atmosphere, pressure, and furnace construction (Demirbas, 2004; Onay, 2007). Inorganic elements that exist indigenously in biomass also influence the characteristics of the pyrolytic products (Wang et al., 2010).

1.2. Effects of inorganic metals on fast pyrolysis of biomass

Biomass consists of about 70% carbohydrates or sugars, 30% lignin, and most species also contain about 5% of a third portion of smaller molecular fragments, called extractives, and inorganic elements. Inorganic elements are the main constituents of ash and their contents range from less than 1% in lignocellulosic biomass to 15% in herbaceous biomass and forestry residues. The inorganic elements are primarily composed of alkali and alkali earth metals such as potassium, calcium, and magnesium (Agblevor and Besler, 1996; Fahmi et al., 2007).

As inorganic elements indigenously exist in biomass, several problems have occurred during the thermal conversion. Specifically, the presence of alkali metals is a potential source of fouling, hot corrosion, and erosion of the turbine blade in power generation systems, as well as fouling in steam boiler tubes (Moses and Bernstein, 1994). In addition, agglomerated particles and slag deposits produced on the surface of the equipment has a harmful effect on the heat-transfer rate and current of the process. The accumulation of ash in the reactor also affects the process efficiency.

Inorganic metals also play a crucial role in the thermal degradation of biomass. With higher inorganic metal content, the maximum decomposition temperature of the biomass is likely to decrease and char formation is promoted (Eom et al., 2012a). Inorganic metals also have an effect on the physicochemical properties of bio-oil including viscosity, water content, and the chemical components due to the induction of secondary cracking during fast pyrolysis (Mourant et al., 2011). Specifically, the amount of levoglucosan, an anhydrosugar formed from carbohydrates, is dramatically decreased by the presence of inorganic metals.

Meanwhile, the bio-oil and bio-char produced from fast pyrolysis contain high levels of inorganic metals because of the inherent inorganic elements in biomass. Inorganic

metals in the pyrolytic products are important for the practical use and storage of the products (Agblevor et al., 1994). However, the transportation mechanism of inorganic material into bio-oil is not known (Agblevor and Besler, 1996).

1.3. Objectives

A fundamental understanding of the relationship between inorganic metals and biomass during fast pyrolysis is lacking. The effects of certain inorganic metals on the composition and properties of bio-oil also remain to be elucidated (Mourant et al., 2011). In addition, many studies focus on the analytical or primary pyrolysis of biomass with inorganic metals rather than on fast pyrolysis, a practical process for the production of bio-oil.

Furthermore, there are only a few reports regarding the distribution of inorganic species in the pyrolytic products from fast pyrolysis and little information exists about the metal distribution within pyrolytic products as a function of temperature (Jendoubi et al., 2011).

For these reasons, this study largely focuses on the effect of inorganic metals on fast pyrolysis and the characteristics of the pyrolytic products. The distribution of inorganic metals in pyrolytic products will also be investigated. First, certain inorganic metals will be impregnated into biomass samples at various concentrations and fast pyrolysis will be carried out at different temperatures to establish the catalytic effects of inorganic metals. Prior to pyrolysis, TGA will be conducted to investigate the thermal decomposition of biomass. Furthermore, inorganic distributions as well as the physicochemical properties of the pyrolytic products will be analyzed by various analytical methods.

2. Literature review

2.1. Fast pyrolysis

2.1.1. Fast pyrolysis and bio-oil

Fast pyrolysis is a thermochemical conversion process commonly considered as the best technology for the production of liquid fuel or bio-oil (Lu et al., 2009). The yields of fast pyrolysis are typically about 60–75 wt% bio-oil, 15–25% bio-char, and 10–20% non-condensable gas. There have been numerous studies regarding the optimal experimental conditions for the production of bio-oil from fast pyrolysis and the analysis of the physicochemical properties of the pyrolytic products (Oasmaa and Peacocke, 2001; Kim et al., 2011; Pittman Jr. et al., 2012). In general, 500°C, a residence time of less than 2 s, and feedstock particle size of less than 3 mm are proper experimental conditions for the production of bio-oil.

Bio-oils are dark brown, free-flowing liquids with an acrid or smoky odor. They consist of a complex mixture of compounds derived from the depolymerization of cellulose, hemicellulose, and lignin. Chemically, they comprise water (15–30 wt%), more or less solid particles (~ <3 wt%), and hundreds of organic compounds including acids, alcohols, ketones, aldehydes, phenols, ethers, esters, sugars, furans, nitrogen-containing compounds, and multifunctional compounds (Milne et al., 1997; Kim et al., 2011). In terms of fuel properties, the viscosity and higher heating values of bio-oil are typically 20–1000 cSt and 17.0 MJ/kg, respectively (Bridgewater, 2004).

2.1.2. Factors on fast pyrolysis

Numerous studies have investigated the different factors that can influence fast pyrolysis. Specifically, the yields and properties of bio-oil are largely affected by the pyrolysis conditions and biomass feedstock.

Fast pyrolysis of woody biomass (yellow poplar) was conducted at various temperatures and residence times to investigate the effect on the yield and characteristics of the pyrolytic products. As a result, the maximum yield of bio-oil was obtained at 500°C and 1.9 s of residence time. The bio-oil and bio-char yields were decreased at higher temperatures and residence times due to secondary cracking. The chemical components of bio-oil, as identified by GC-MS, were also altered depending on the experimental conditions. As the temperature and residence time of the pyrolysis increased, the amount of carbohydrate-derived compounds and lignin-derived compounds increased (Kim et al., 2011).

Additionally, the fast pyrolysis of different biomass feedstock (sweetgum, switchgrass, and corn stover) was performed in an auger-fed reactor at 450 °C and the produced bio-oils were characterized. Of the three feedstock solutions, sweetgum produced higher (or comparable) bio-oil yields than switchgrass and corn stover. This was attributed to the higher carbohydrate and lignin content, as well as lower ash content of sweetgum as compared to the other feedstock (Wang et al., 2012).

2.2. Effect of inorganic metals on thermal decomposition of biomass

2.2.1. Comparing raw and demineralized biomass

Biomass contains significantly higher amounts of inorganic metals than other fuels such as coal and petroleum. The inorganic metals released during the pyrolysis of biomass may act as catalysts. Therefore, numerous investigations have focused on the effects of inorganic metals on the pyrolysis of biomass. In order to confirm the general effect of inorganic metals in biomass, they were removed by various methods. Then, the thermal decomposition behaviors and properties of the pyrolytic products were investigated and the raw and demineralized biomasses were compared.

According to Eom et al. (2011), inorganic metals affected the thermal behavior of biomass, as analyzed by TGA and analytical pyrolysis. Poplar wood powders were treated with D.I. water, tap water, HCl, and HF to remove the inorganic metals. The maximum degradation temperature increased following the removal of inorganic metals. The total amount of low molecular weight compounds such as acetic acid and 3-hydroxypropanal was dramatically lowered in demineralized samples, while levoglucosan increased 2–10-fold.

In another study, mallee wood was washed with water and a dilute solution of acid to remove the inorganic elements. The water- and acid-washed samples were then pyrolyzed in a fluidized-bed reactor at 500°C. Inorganic metals did not significantly affect the yields of bio-oil and bio-char, but the bio-oil properties were drastically altered. For instance, the viscosity of the bio-oil decreased from 200 mPas to 50 mPas after the removal of the inorganic metals. In addition, the amount of mono-phenols in the bio-oil increased, whereas the amount of pyrolytic sugars decreased as the amount of inorganic metals in the biomass increased (Mourant et al., 2011).

2.2.2. Catalytic effects of specific inorganic metals

The species and amount of inorganic elements is inherently diverse in different biomass samples, thus investigation of the catalytic effects of different types of inorganic metals is warranted. Among various inorganic metals such as K, Ca, Mg, and Na, K (potassium) has the greatest influence on the thermal conversion of biomass (Nowakowski et al., 2007; Fahmi et al., 2008; Eom et al., 2012a).

In order to examine the effects of different inorganic metals, K, Mg, and Ca were impregnated into poplar wood powder at various concentrations and the pyrolysis of each sample was investigated using TGA and Pyroprobe-GC-MS. As a result, when the potassium content increased, the char formation increased from 10.5 wt% to 19.6 wt% at 550 °C. Furthermore, the temperature at which the maximum degradation rate was achieved shifted from 367 °C to 333 °C. With increasing magnesium content, the maximum degradation rate increased from 1.21 wt%/°C to 1.43 wt%/°C. Further, potassium had a distinguishable catalytic effect on the suppression of levoglucosan formation, whereas levoglucosan formation gradually increased with magnesium. Unlike potassium and magnesium, calcium did not induce significant changes in the formation of the pyrolytic compounds.

Furthermore, potassium-catalyzed cell-wall components (cellulose, hemicellulose, and lignin) were analyzed by TGA and Py-GC-MS to observe the effect of potassium on each cell-wall component. Potassium influenced all components, as the maximum degradation temperature decreased. Potassium also affected lignin pyrolysis by catalyzing polymerization reactions so that the char yield increased from 37% to 51%.

3. Materials and methods

3.1. Materials

Yellow poplar wood (*Liriodendron tulipifera*: YP) was used in this experiment as the raw lignocellulosic biomass and was kindly provided by the Korea Forest Research Institute (Seoul, Republic of Korea). The size of the biomass was approximately 0.5 mm. The wood sample was dried in an oven at 75°C overnight prior to pyrolysis, and the final moisture content of the sample was ~2 wt%.

3.2. Demineralization and impregnation of inorganic metals

Inorganic metals in biomass were removed by washing with dilute hydrofluoric acid (HF, Extra pure grade purchased from Duksan). The sample was prepared by stirring a mixture of 3 wt% HF solution and 100 g of YP wood powder at 400 rpm for 1 h at room temperature. The biomass sample was then rinsed with deionized water and dried at 75°C overnight.

To impregnate the potassium and magnesium, KCl (≥99.0%, powder) and $MgCl_2$ (anhydrous, ≥98%) obtained from Sigma-Aldrich were used. HF-treated yellow poplar (HF-YP) was immersed in a solution of KCl or $MgCl_2$ in the ratio of 10 mL per gram of biomass with increasing salt concentrations (0, 0.5, 1.0, and 2.0 wt%). Each mixture was stirred at 200 rpm for 48 h at room temperature. After stirring, the sample was filtered and dried in an oven at 75°C overnight. The biomass sample treated with 0 wt% salt was called demineralized YP (D-YP) and the others were called K-0.5, K-1.0, and K-2.0 depending on the concentration of potassium added into the mixture. The Mg-impregnated samples were named in a similar fashion (i.e., Mg-0.5, Mg-1.0, and Mg-2.0).

3.3. Fast pyrolysis experimental setup and procedure

Fast pyrolysis was performed on the raw and inorganic metal-impregnated samples using a fluidized bed fast pyrolyzer (Figure 1). Pyrolytic products (bio-char, bio-oil, and non-condensable gasses) were obtained at different temperatures (450, 500, and 550°C) and each process was carried out in duplicate. The flow rate of purified nitrogen purged into the reactor to establish inert atmospheric conditions was 10 L/min and the residence time was calculated to be 1.25 s. The bio-oil and bio-char, target products for analysis in this study, were recovered from each collector and the yield of wet pyrolytic products was calculated as follows:

$$\text{Yield of bio-oil} = \frac{\text{Bio-oil (g)}}{\text{Biomass}} \times 100 \quad (1)$$

$$\text{Yield of bio-char} = \frac{\text{Bio-char (g)}}{\text{Biomass}} \times 100 \quad (2)$$

$$\text{Yield of gas} = 100 - (\text{yield of bio-oil} + \text{yield of bio-char}) \quad (3)$$

In addition, two extracting bottles filled with acetone were connected to the electrostatic precipitator (Figure 1). The non-condensable gas fraction formed during pyrolysis was passed through the bottles in order to extract acetone-soluble pyrolytic products contained in the non-condensable gas. These products were called “non-condensed pyrolytic compounds”. Overall process of fast pyrolysis is given in Figure 2.

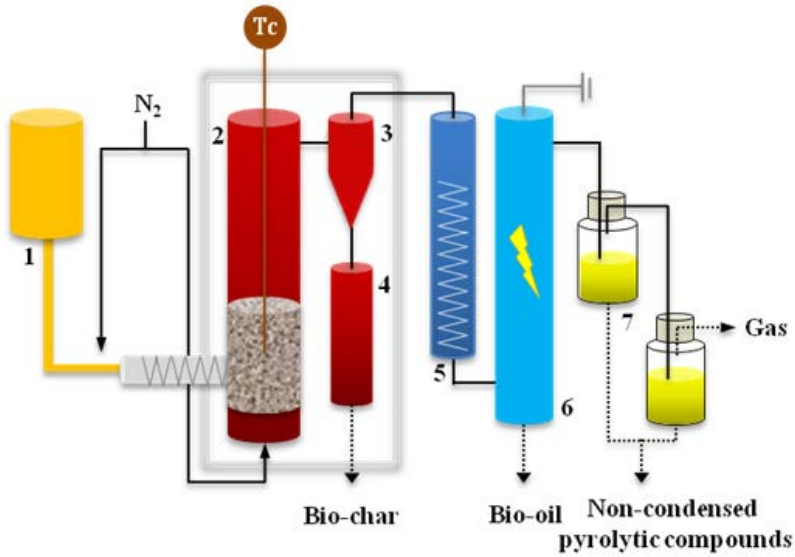

Figure 1 Fluidized bed fast pyrolysis system with two acetone filters (1: feeder, 2: reactor, 3: cyclone, 4: char collector, 5: cooler, 6: electrostatic precipitator, 7: extractors filled with acetone).

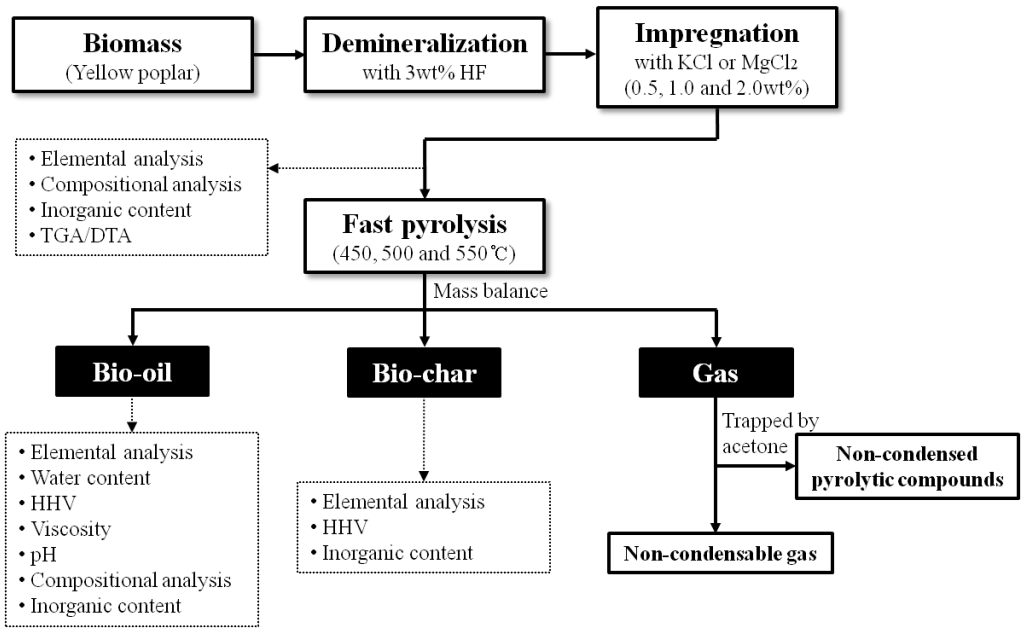

Figure 2 Overall process.

3.4. Analysis

3.4.1. Elemental and component analysis

Elemental analysis (C, H, and N) was performed using a US/CHNS-932 (LECO Corp., USA) and the oxygen content was calculated by the difference. The holocellulose (the sum of cellulose and hemicellulose), lignin, and ash content in the biomass samples were determined according to the method presented by NREL (National Renewable Energy Laboratory) (Sluiter et al., 2004; Sluiter et al., 2005).

3.4.2. TG/DTG analysis

Prior to fast pyrolysis, the thermal decomposition of the raw and inorganic metal-impregnated samples was determined by thermogravimetric and differential thermogravimetric analysis (TG and DTG analysis) using a Q-5000 IR instrument (TA Instrument, USA). Samples (ca. 3.5 mg) were heated under N_2 gas flow at a heating rate of 10°C/min in the range 40–800°C.

3.4.3. Inorganic metal content of biomass and pyrolytic products

In order to quantify the amounts of the inorganic elements in the biomass samples after demineralization and impregnation, ICP-ES (inductively coupled plasma-emission spectrometer) analysis was performed. Weighed samples (around 0.5 g) were digested with 10 mL of a mixture of HNO_3:HCl:H_2O_2 (8:1:1, v/v) using a microwave (Mutiwave 3000, Anton Paar). After digestion, the samples were diluted with 50 mL purified water and filtered with Whatman No. 42 filter paper. The samples were then analyzed using an ICPS-1000IV instrument (Shimadzu, Japan).

To determine the behavior of inorganic metals on fast pyrolysis, their distribution in the pyrolytic products was observed by quantifying the inorganic content of the bio-oil and bio-char according to the method described above. Since some sand (the fluidized bed material in the pyrolyzer) passed over into the char collector during fast pyrolysis, bio-char mixed with sand and was difficult to separate. Accordingly, ICP-ES analysis of sand was also performed as a control for sand-mixed bio-char and then the inorganic content of bio-char was calculated considering the amount of inorganic metals derived from sand using the weight of sand in each mixture.

3.4.4. Water content, viscosity, acidity, and HHV of pyrolytic products

The water content of the bio-oil from potassium-impregnated biomass was determined by Karl-Fischer titration (ASTM E203; DAIHAN, Korea) and by 870 KF Titrino plus (Radiometer, Switzerland) for bio-oil from magnesium-impregnated biomass. The viscosity and acidity of the bio-oil was measured using a capillary-type viscometer at 40°C and a pH meter (Thermo Fischer Scientific Inc., USA), respectively. The higher heating values (HHV) of bio-oil and bio-char were estimated according to the correlation (Eq. 4) by Sheng and Azevedo (Sheng and Azevedo, 2005):

$$HHV = -1.3675 + 0.3137 \times C + 0.7009 \times H + 0.0318 \times O \quad (4)$$

3.4.5. GC–MS analysis of bio-oil

Gas chromatography–mass spectrometry (GC-MS) was performed to identify chemical compounds in bio-oil and non-condensed pyrolytic compounds dissolved in the acetone trapper. First, in order to analyze the bio-oil, the samples (0.45 mL) were diluted in 0.5 mL of acetone with an added internal standard of 0.05 mL fluoranthene. Quantitative determination was conducted using a gas chromatograph (Agilent 7890A) equipped with a flame ionization detector (FID) and a DB-5 capillary column (60 m × 0.25 mm × 0.25 μm) for bio-oil from potassium-impregnated biomass and non-condensed pyrolytic compounds. A gas chromatograph (Agilent 7890B) equipped with a FID and a DB-5 capillary column (30 m × 0.25 mm × 0.25 μm) was utilized to analyze bio-oil from magnesium-impregnated biomass. The oven was programmed to maintain 50°C for 5 min, ramp at 3°C/min to 280°C, and hold at 280°C for 10 min. The injector and FID detector temperatures were 250°C and 300°C, respectively, and the injector split ratio was set at 20:1. The compounds in bio-oil were qualified using a mass selective detector (Agilent 5975C) with the NIST (National Institute of Standards and Technology) mass spectral library. For quantitative analysis, response factors (Rf) determined in a previous study (Eom et al., 2012b) were used selectively and the Rf values of the other compounds were semiquantitatively estimated based on structural similarities.

3.4.6. Solid content of bio-oil

The solid content of bio-oil was determined according to a modified version of VTT of Finland (Oasmaa and Peacocke, 2001). Bio-oil was diluted with ethanol (5 : 1 = ethanol : bio-oil (w/w)) and then filtered using a 20–25 μm filter (Wattman no. 41) and a 0.50 μm syringe filter in sequence. Solids with diameters greater than 20–25 μm

were obtained from the first filtration and solids in the range varying from 0.50 to 20–25 μm were obtained from the second filtration. Their content was calculated on a wet basis and referred to as larger particles (LP; from the first filtration) and smaller particles (SP; from the second filtration).

3.4.7. GPC analysis of bio-oil

The average molecular weights of the bio-oils were measured using a gel permeation chromatography (GPC) max instrument (Viscotek RImax, Viscotek, UK) coupled with a UV-Vis detector (VE3210, Viscotek) equipped with PLgel 5 μm MIXED-C columns (300 mm × 7.5 mm, Varian, Inc.). Each sample (ca. 2 mg) was dissolved in tetrahydrofuran and filtered to remove any insoluble solids. Polystyrenes were used as the standards to create a calibration curve.

4. Results and discussion

4.1. Characteristics of biomass samples

Elemental and component analysis of the raw and inorganic metal-impregnated biomass samples are given in Table 1. The removal of inorganic metals by HF did not result in any significant changes in the biomass structure or composition. On the other hand, the ash content of each sample increased in proportion to the concentration of impregnated potassium or magnesium.

Figure 3 shows the concentrations of inorganic elements in YP before and after inorganic metal-impregnation. For the raw biomass samples, more than 90 wt% of the total inorganic elements consisted of potassium, magnesium, and calcium (referred to as alkali and alkali earth metals). As shown in Figure 3, the inorganic elements, especially alkali and alkali earth metals, were effectively removed by HF and DI water whereas most of the others remained. However, more than half of the initial content of calcium remained. This result indicated that calcium interacted strongly with the biomass and thus was difficult to remove using mild conditions. Potassium and magnesium were effectively removed and then impregnated in biomass at various concentrations.

Table 1 Chemical composition of raw and inorganic metal-impregnated biomass.

	Elemental analysis (wt.%)				Holocellulose (wt.%)	Lignin (wt.%)	Ash (wt.%)
	C	H	N	O[a]			
YP[b]	45.8	5.8	0.2	48.2	74.0	30.0	0.45
D-YP[c]	47.1	6.1	0.1	46.7	72.1	29.2	0.17
K-0.5[d]	46.4	6.3	0.1	47.2	74.1	30.0	0.22
K-1.0[d]	47.2	6.2	0.1	46.5	74.1	28.2	0.26
K-2.0[d]	46.9	6.3	0.1	46.7	75.0	29.1	0.37
Mg-0.5[d]	46.6	6.2	0.2	47.1	73.2	27.9	0.48
Mg-1.0[d]	46.0	6.1	0.2	47.6	72.8	28.1	0.55
Mg-2.0[d]	46.5	6.0	0.2	47.3	73.2	28.0	0.62

[a] by difference.
[b] Yellow poplar.
[c] Demineralized yellow poplar.
[d] Inorganic metal-impregnated samples with concentrations of KCl or $MgCl_2$ 0.5, 1.0, 2.0 wt.%, respectively.

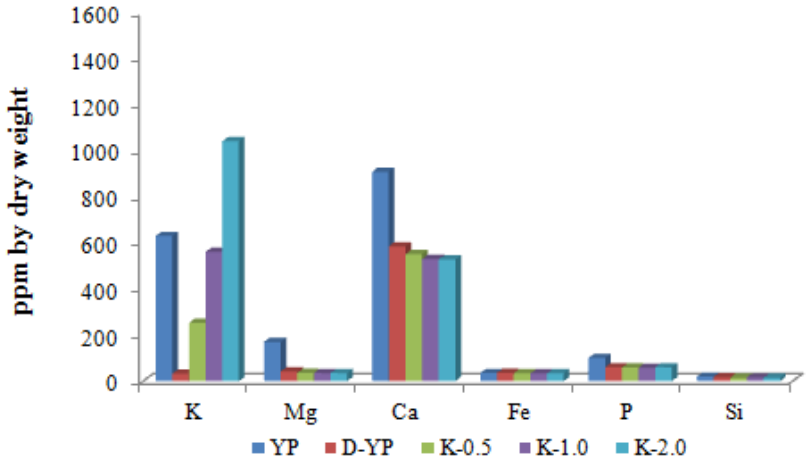

Figure 3 Contents of inorganic elements in potassium-impregnated biomass samples.

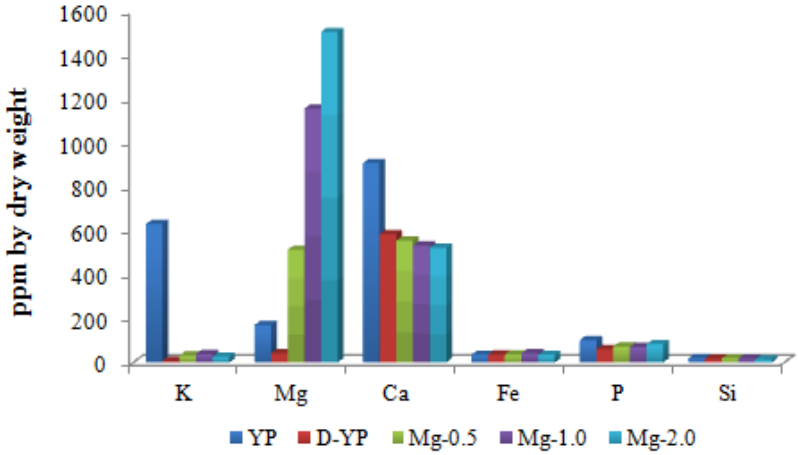

Figure 4 Contents of inorganic elements in magnesium-impregnated biomass samples.

4.2. Thermal decomposition of biomass samples

TGA and DTG results comparing the effect of inorganic metals in biomass samples are shown in Figures 5 and 6 and Tables 2 and 3. A two-step thermal degradation of the biomass was revealed by the DTG curves (Figures 5 and 6). The first weight loss was observed at approximately 300°C followed by the second weight loss at 370°C; these were attributed to the decomposition ranges of hemicellulose and cellulose, respectively (Nowakowski and Jones, 2008).

As the potassium and magnesium content of the biomass increased, the first peak gradually disappeared and the overall DTG curves shifted to lower temperatures. These results indicated that inorganic metals allowed the thermal decomposition of biomass to occur at lower temperatures than the D-YP due to their catalytic effects (Kowalski and Wokaun, 2007; Nowakowski et al., 2007). In addition, the DTG curve of the magnesium-impregnated biomass (Figure 6) showed the diminished first peak and a narrower decomposition range than D-YP, which suggested that magnesium significantly influenced the decomposition of hemicelluloses and the initial decomposition of cellulose.

Detailed TGA and DTG data are summarized in Table 2 and 3. After the overall process was finished at 800°C, 93.2 wt% of YP was volatilized and 6.8 wt% was converted to char. Potassium significantly increased the char yield from 4.4% to 9.1%, whereas the volatile yield decreased from 95.6% (D-YP) to 90.9% (K-2.0). The char yield of the biomass increased with magnesium, but not as much as with potassium despite the higher amount of magnesium in Mg-2.0 as compared to the amount of potassium in K-2.0. Therefore, a relatively small amount of potassium had a larger influence on the char yield as compared to magnesium.

The maximum decomposition temperature increased from 356.6°C to 373.9°C after the removal of the inorganic metals in the biomass. It decreased to 359.0°C as the

impregnated concentration of potassium increased. This result indicated that potassium had an effect on the thermal stability of the biomass as a catalyst of the decomposition reaction. Meanwhile, the maximum decomposition temperature decreased to 337.6°C as the magnesium content increased. This could be attributed to the fact that the degree of polymerization (DP) of cellulose was reduced due to the altered reactivity of the surface molecules by binding with magnesium (Shimada et al., 2008).

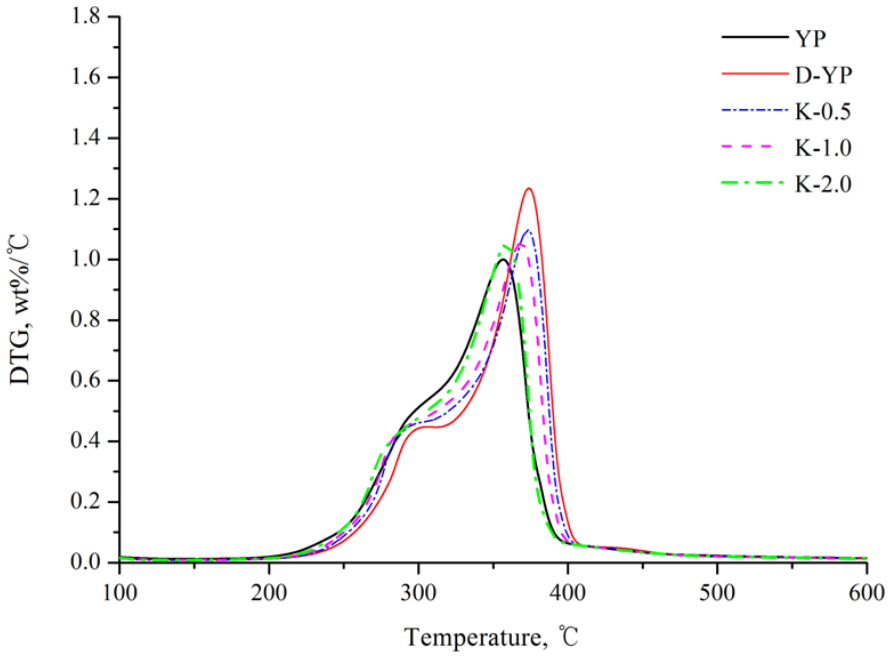

Figure 5 DTG curves of raw and potassium-impregnated biomass (10°C/min).

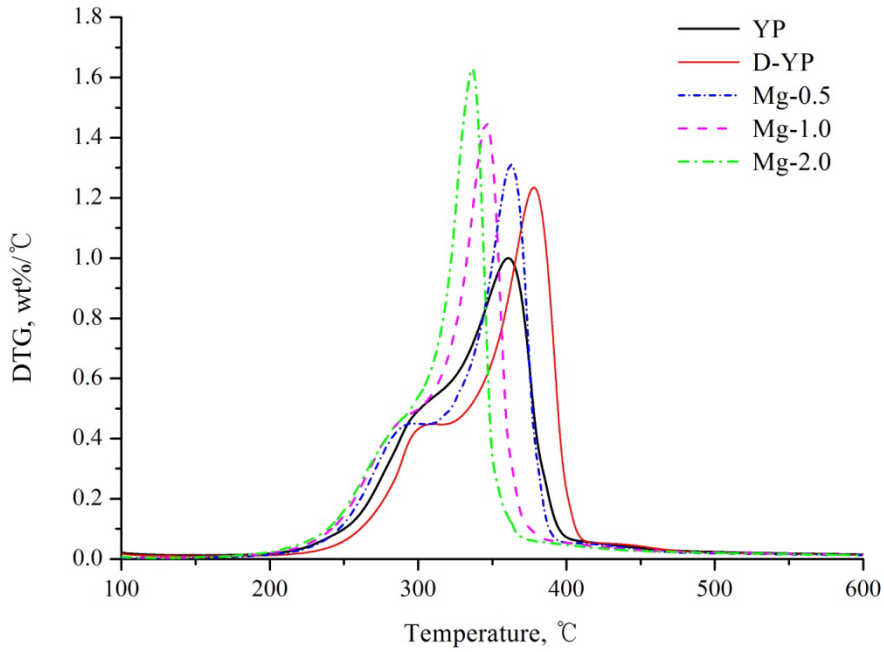

Figure 6 DTG curves of raw and magnesium-impregnated biomass (10°C/min).

Table 2 Pyrolysis properties of potassium-impregnated biomass by TG and DTG in N_2 at heating rate of 10°C/min.

	Yield (wt.%)		Max. degradation rate (wt.%/°C)	Temperature at max. rate (°C)
	Volatiles	Char		
YP	93.2	6.8	1.00	356.6
D-YP	95.6	4.4	1.24	373.9
K-0.5	93.7	6.3	1.10	373.1
K-1.0	93.4	6.6	1.06	368.4
K-2.0	90.9	9.1	1.05	359.0

Table 3 Pyrolysis properties of magnesium-impregnated biomass by TG and DTG in N_2 at heating rate of 10°C/min.

	Yield (wt.%)		Max. degradation rate (wt.%/°C)	Temperature at max. rate (°C)
	Volatiles	Char		
YP	93.2	6.8	1.00	356.6
D-YP	95.6	4.4	1.24	373.9
Mg-0.5	95.6	4.4	1.31	364.2
Mg-1.0	94.4	5.6	1.45	345.8
Mg-2.0	92.6	7.4	1.63	337.6

4.3. Recovery of pyrolytic products

4.3.1. Yields of pyrolytic products

Tables 4 and 5 show the yields of the pyrolytic products from the fast pyrolysis of raw and impregnated biomass samples. The highest yield of bio-oil, ~59.7%, was obtained at 450°C and the yield was more influenced by the pyrolysis temperature rather than the inorganic content in the biomass.

The yields of the bio-oil from potassium-impregnated biomass at 450°C and 500°C decreased due to certain issues during the fast pyrolysis. Under those conditions (450°C, 500°C, and potassium-impregnated samples), flocculated char was obtained rather than loose particles, which is the general form of char obtained from the fast pyrolysis of lignocellulosic biomass. Moreover, the char was present in the pyrolysis reactor, not in the char collector. The proportion of char recovered from the reactor was approximately 57–98% for potassium-impregnated samples, as compared to about 4% for YP under the same conditions. This might lead to subsequent problems such as the deterioration of the fluidization conditions and heat transfer rates, which are closely related to the residence time and conversion efficiency of the volatiles. Thus, the yields of bio-oil under those conditions varied due to the instability during the fast pyrolysis caused by the agglomeration of char in the reactor. Conversely, fast pyrolysis at 550°C ran smoothly for all samples because the high temperature led to a decreased amount of char formation.

Agglomeration of char induced by inorganic metals has been previously reported (Skrifvars et al., 1998). When inorganic metals are released, they react with accessible surfaces like fluidized bed materials such as silica, and form low-melting eutectic mixtures of inorganic metals and silica. A liquid layer on the bed-material particles would tend to induce agglomeration. Additionally, char formation reactions were

largely influenced by potassium in this study. The char yield increased with increased potassium content and the yield in the case of K-2.0 was almost double compared to that of D-YP at all temperatures. These data were in agreement with the results of TG/DTG analysis. As the temperature increased, however, the char yield decreased and the gas yield increased due to secondary cracking reactions promoted at high temperatures (Bridgwater et al., 1999; Kim et al., 2011).

Magnesium also had an influence on the char formation. Agglomeration of char proceeded with high magnesium contents, but the char did not prevent the flow of volatiles or gaseous compounds during pyrolysis. Thus the oil yield was not significantly altered, and the char yield slightly increased (Table 5). It is known that inorganic metals can play a catalytic role in char formation, though this influence is not completely understood (Nowakowski et al., 2007; Nowakowski and Jones, 2008; Patwardhan et al., 2010). It could be attributed to the recombination of decomposed volatile fractions favored by inorganic metal ions via an ionic mechanism. Magnesium in biomass would be converted to magnesium oxide in char and then act as an in situ template for the generation of a porous structure, resulting in a large pore volume and surface area of the char (Morishita et al., 2010; Liu et al., 2013). For this reason, the char would have weak bonds that would easily react and break. Therefore, the char yield was less enhanced by magnesium as compared to potassium.

Table 4 Yield of pyrolytic products from raw and potassium-impregnated biomass under various pyrolysis temperatures.

	Yields of pyrolysis products (wt.%)								
	Bio-oil			Bio-char			Gas		
	450°C	500°C	550°C	450°C	500°C	550°C	450°C	500°C	550°C
YP	59.7	52.6	46.8	9.6	8.4	5.8	30.7	39.0	47.5
D-YP	59.6	55.5	46.7	6.2	4.7	3.3	34.2	39.8	50.0
K-0.5	55.3	53.1	45.7	8.1	5.6	5.3	36.7	41.3	48.9
K-1.0	49.8	46.1	44.6	8.5	7.0	6.8	41.7	46.9	48.6
K-2.0	49.3	50.0	48.1	12.1	8.5	7.3	38.7	41.5	44.6

Table 5 Yield of pyrolytic products from raw and magnesium-impregnated biomass under various pyrolysis temperatures.

	Yields of pyrolysis products (wt.%)								
	Bio-oil			Bio-char			Gas		
	450°C	500°C	550°C	450°C	500°C	550°C	450°C	500°C	550°C
YP	59.7	52.6	46.8	9.6	8.4	5.8	30.7	39.0	47.5
D-YP	59.6	55.5	46.7	6.2	4.7	3.3	34.2	39.8	50.0
Mg-0.5	53.3	56.7	45.9	8.1	5.1	5.1	38.6	38.2	49.0
Mg-1.0	54.0	52.3	47.2	8.2	6.7	6.2	37.8	41.0	46.6
Mg-2.0	55.8	54.8	44.6	8.5	7.7	7.0	35.7	37.5	48.4

4.3.2. Analysis of non-condensed pyrolytic compounds

Nine non-condensed pyrolytic compounds were identified from the gas fraction of fast pyrolysis and their GC-MS chromatograms and structural formulas are shown in Figure 7. It is well known compounds a, c, d, and f in Figure 7 are derived from carbohydrates following pyrolysis (Faix et al., 1991). Compounds b, e, g, h, and i are aromatic hydrocarbons, commonly called BTEXS (benzene, toluene, ethylbenzene, xylenes, and styrene), and are utilized as valuable commodity chemicals (Vispute et al., 2010). Due to their aromatic structure, BTEXS are assumed to be derived from lignin via demethoxylation and side chain cleavage (Faix et al., 1990; Nowakowski and Jones, 2008). However, those compounds were rarely reported as chemical components of bio-oil produced from lignocellulosic biomass. From this research, it is clear that BTEXS were formed during the fast pyrolysis of lignin, although their concentrations were low and they did not condense to the liquid form of bio-oil under the condensation system (cooler and electrostatic precipitator).

The inability of BTEXS to condense could be explained by their structural features (related to the electronegativity of the compounds). All chemical compounds identified in bio-oil have functional groups such as hydroxyl, methoxyl, or carbonyl groups whereas BTEXS do not. In the fast pyrolysis, volatiles immediately pass through the cooler and electrostatic precipitator. Most of the volatiles turn into bio-oil during this process, while BTEXS, which are unable to become bio-oil, pass through and are dissolved in acetone. Quantitative analysis of BTEXS compounds will be performed in future studies.

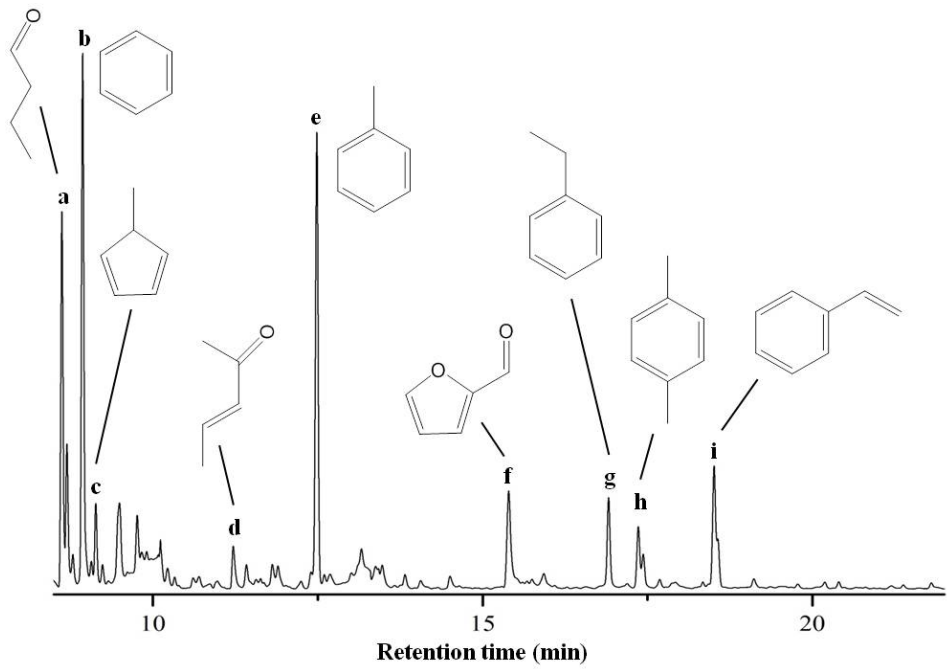

Figure 7 GC-MS chromatogram for non-condensed pyrolytic compounds trapped in acetone. Major peaks are identified by mass spectra as follows: (a) 2-Butenal; (b) Benzene; (c) 5-Methyl-1,3-cyclopentadiene; (d) 3-Penten-2-one; (e) Toluene; (f) Furfural; (g) Ethylbenzene (h) p-Xylene (i) Styrene.

4.4. Effect of potassium on the characteristics of pyrolytic products

4.4.1. Physicochemical properties of pyrolytic products

Table 6 and 7 show the physicochemical properties of bio-oil and bio-char from raw and potassium-impregnated samples. The carbon and oxygen content in the bio-oil ranged from 44.7% to 47.0% and 45.8% to 47.7%, respectively. As the potassium content increased from D-YP to K-2.0, the amount of carbon in the bio-oil slightly decreased while the amount of oxygen increased at all temperatures. Contrary to bio-oil, the amount of carbon in bio-char increased while the amount of oxygen decreased. This was a result of the dehydration reaction during fast pyrolysis and the carbon crystallization of bio-char enhanced by the potassium-oxygen interaction to form carbon monoxide (Tsubouchi et al., 2003). In addition, an increase in the carbon content of bio-char was observed as the pyrolysis temperature increased. This increase was a result of the breaking of weaker bonds within the bio-char structure at high temperatures, which led to a loss of hydrogen and oxygen (Demirbas, 2004).

The HHV of bio-oil was estimated to be 19.2–19.7 MJ/kg, which was lower than that of heavy oil (45 MJ/kg) from fossil fuel. They could be improved by an upgrading process such as hydrodeoxygenation, catalytic cracking, and emulsification (Bridgwater, 2012). The HHV of the bio-char, however, was estimated to be 24.5–26.9 MJ/kg, which was similar to that of coal (25 MJ/kg). The pH of the bio-oil varied from 2.2 to 3.1. The acidity of the bio-oil was due to several acids (e.g., acetic acid) that were formed during pyrolysis (Lu et al., 2009). In general, the acidity of the bio-oils did not change significantly, indicating that potassium had little effect on the acidity.

As shown in Figure 8, a high potassium content in the biomass resulted in a high water content of the bio-oil. It was reported that dehydration reactions occur in free

hydroxyl groups and carboxylic groups in carbohydrates when potassium acts as a Lewis acid (Wang et al., 2010). Jakab et al. also suggested that dehydration was promoted by the addition of alkali metals from terminal hydroxyl and aldehyde groups in lignin (Jakab et al., 1993). Alkali metal ions were likely to be released by involving a hydroxyl group and a hydrogen atom from a near carbon to form a alkali metal ion-water complex ($H_2O \cdot M^+$, M: alkali metal) during the pyrolysis. This transition state would lead to dehydration as the product was more stable (Nimlos et al., 2003). Consequently, potassium could induce dehydration reactions during the decomposition of the biomass.

Moreover, these potassium-induced dehydration reactions seemed to be increasingly activated as the temperature increased. For instance, the water content increased from 14.4 wt% in D-YP to 16.1 wt% in K-2.0 at 450°C, while it increased from 14.4 wt% to 19.7 wt% at 550°C. Activation of potassium as a catalyst as a function of temperature could be explained by the release behavior of potassium at different temperatures (as described in Section 4.6).

The viscosity of bio-oil (Figure 9) varied from 16 cSt to 45 cSt despite the increase in the water content. Highly viscous bio-oil was produced when inorganic metals were removed and the pyrolysis temperature was lower.

Table 6 Physicochemical properties of bio-oil and bio-char obtained from raw and demineralized biomass.

	Temperature (˚C)					
	450		500		550	
Sample	YP	D-YP	YP	D-YP	YP	D-YP
Bio-oil						
Elemental analysis (%)						
Carbon	46.9	46.5	46.2	46.7	46.1	47.0
Hydrogen	6.9	6.9	7.3	7.0	6.7	7.0
Nitrogen	0.2	0.2	0.2	0.2	0.2	0.2
Oxygen*	46.0	46.4	46.3	46.1	47.0	45.8
HHV(MJ/kg)	19.6	19.5	19.7	19.7	19.3	19.7
pH	2.9	2.5	3.0	2.6	3.1	2.6
Bio-char						
Elemental analysis (%)						
Carbon	74.6	77.5	75.4	75.8	80.3	79.2
Hydrogen	3.6	2.1	3.2	3.2	3.0	2.8
Nitrogen	0.5	0.7	0.5	1.2	0.5	0.9
Oxygen*	21.3	19.7	20.9	19.8	16.2	17.1
HHV(MJ/kg)	25.2	25.0	25.2	25.3	26.4	26.0

*by difference

Table 7 Physicochemical properties of bio-oil and bio-char obtained from potassium-impregnated biomass.

	Temperature (˚C)								
	450			500			550		
Sample	K-0.5	K-1.0	K-2.0	K-0.5	K-1.0	K-2.0	K-0.5	K-1.0	K-2.0
Bio-oil									
Elemental analysis (%)									
Carbon	46.3	44.9	44.7	46.4	45.4	45.0	46.3	45.3	45.0
Hydrogen	6.6	7.2	7.5	7.0	6.9	7.1	7.3	7.5	7.4
Nitrogen	0.2	0.2	0.2	0.2	0.1	0.2	0.3	0.2	0.3
Oxygen*	46.9	47.7	47.6	46.4	47.6	47.7	46.1	47.0	47.3
HHV(MJ/kg)	19.3	19.3	19.4	19.6	19.2	19.2	19.7	19.6	19.4
pH	2.6	2.5	2.2	2.7	2.6	2.4	2.7	2.6	2.3
Bio-char									
Elemental analysis (%)									
Carbon	79.7	77.6	78.1	75.0	79.8	81.7	81.7	79.5	81.4
Hydrogen	3.4	2.7	3.5	2.3	3.3	3.1	1.1	3.0	2.4
Nitrogen	0.5	0.4	0.4	0.3	0.6	0.4	1.3	0.8	0.5
Oxygen*	16.4	19.3	18.0	22.4	16.3	14.8	15.9	16.7	15.7
HHV(MJ/kg)	26.5	25.5	26.2	24.5	26.5	26.9	25.5	26.2	26.3

*by difference

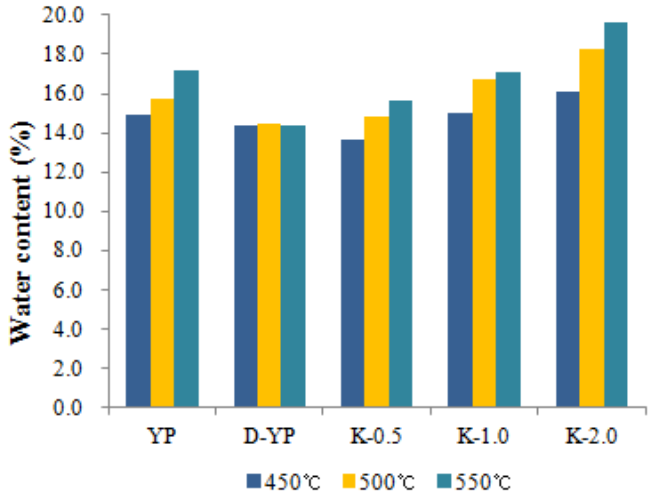

Figure 8 Water content of bio-oil produced under various conditions of potassium content and pyrolysis temperature.

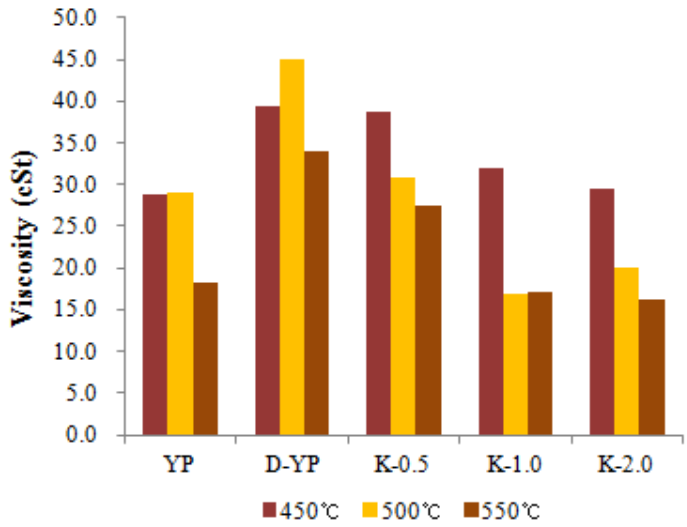

Figure 9 Viscosity of bio-oil produced under various conditions of potassium content and pyrolysis temperature.

4.4.2. Chemical compounds in bio-oil

The composition of bio-oil with various concentrations of impregnated potassium had an effect on the properties of the bio-oil. A total of 44 compounds were identified in the bio-oil (Table 8). As shown in Figure 10, the distribution of chemical compounds between D-YP and K-2.0 were significantly different. The peaks after compound No. 36, which were related to lignin derived compounds, disappeared for D-YP whereas the peak for levoglucosan (No. 35) was remarkably increased. With increased potassium content, the former appeared and the latter gradually decreased. The compounds in the bio-oils produced from raw and potassium-impregnated biomass samples were grouped by their structural characteristics. Specifically, the carbohydrate-derived compounds included levoglucosan (35), cyclopentenes (6, 7, 9, 14), furans (4, 5, 8, 10, 11, 15), and acetic acid (1), while the lignin-derived compounds included syringol-related compounds (27, 32, 36, 37, 39, 40, 42, 44), guaiacol-related compounds (18, 20, 24, 26, 28, 29, 31, 33, 34, 38, 41, 43), catechols (21, 23, 25, 30), and phenols (13, 16, 17, 19, 22; numbers from Table 8); the amounts of each group are shown in Figure 11. The effects of potassium on the bio-oil composition, especially levoglucosan, are described below.

Several studies suggested that the bonds between inorganic metals and oxygen-containing functional groups in biomass could function as bridges (Chaiwat et al., 2008; Mourant et al., 2011). Thus, intermolecular cross-links form and affect the thermal decomposition of biomass. Mourant et al. determined that an extended holding time would promote secondary cracking and condensation reactions by reformation of the bonds between inorganic metals and biomass components (Mourant et al., 2011).

Furthermore, the conjugated structure could decompose to smaller fractions by the accelerated intramolecular cleavage of its binding sites, such as the dehydration reactions mentioned in Section 4.4.1. Subsequently, ring-opened and broken structures would undergo decomposition or recombine with released potassium leading to

secondary reactions. On the other hand, a small amount of potassium in biomass would result in fewer cross-links in the biomass structure. Cleavage of intermolecular bonds, such as glycosidic linkages, would likely occur and larger fractions would be released accordingly.

Therefore, a higher amount of levoglucosan, an anhydrosugar formed by the cleavage of glycosidic linkages, was produced from the bio-oil with the least amount of potassium. However, levoglucosan was decomposed via interactions with potassium and smaller amounts were present in the bio-oil of K-2.0 (Figure 11 (a)). For instance, the amount of levoglucosan decreased from 119.38 mg/g in D-YP to 21.21 mg/g in K-2.0 at 450°C. In addition, the amount of guaiacol-related compounds dramatically increased while the amount of syringol-related compounds slightly increased with increased potassium (Figure 11 (b)). These results indicated that the demethoxylation from an aryl group of lignin was enhanced by potassium during pyrolysis (Jakab et al., 1993).

Temperature also influenced the composition of the bio-oil. Small fractions of carbohydrates and lignin increased at high temperatures (Figure 11). As the temperature increased from 450°C to 550°C, the amount of guaiacol-related compounds increased from 2.25 mg/g to 8.59 mg/g in D-YP and from 5.90 mg/g to 12.74 mg/g in K-2.0. On the contrary, syringol-related compounds decreased from 3.29 mg/g to 1.56 mg/g in D-YP and from 4.89 mg/g to 3.58 mg/g in K-2.0. The results indicated that demethoxylation could also be facilitated by higher temperatures.

Table 8 Comparison of concentration of chemical compounds in bio-oil pyrolyzed from potassium-impregnated biomass at 450°C.

No.	Source	Compound	Concentration (mg/g biomass)				
			YP	D-YP	K-0.5	K-1.0	K-2.0
1	C[a]	Acetic acid	35.78	36.71	37.05	35.03	43.55
2	C	1-hydroxy-2-Propanone	1.90	2.42	1.79	1.42	2.34
3	C	3-hydroxy-2-Butanone	0.20	1.74	0.31	0.23	0.14
4	C	3-Furaldehyde	0.34	0.49	0.32	0.25	0.23
5	C	Furfural	5.54	4.97	3.98	5.80	6.26
6	C	2-Cyclopentene-1,4-dione	0.60	0.21	0.60	0.62	0.28
7	C	2-metyl-2-Cyclopenten-1-one	0.50	0.65	0.38	0.38	0.42
8	C	2(5H)-Furanone	9.94	2.60	1.08	9.52	9.08
9	C	1,2-Cyclopentanedione	1.81	2.06	3.08	1.99	4.72
10	C	5-metyl-2(5H)-Furanone	0.71	0.51	0.76	0.65	0.73
11	C	5-methyl-2-Furancarboxaldehyde	0.82	0.99	0.80	0.82	1.10
12	C	2H-Pyran-2-one	0.29	0.55	0.37	0.32	0.25
13	L[b]	Phenol	0.21	0.35	0.31	0.25	0.28
14	C	3-methyl-1,2-Cyclopentanedione	1.61	0.86	0.98	1.17	1.36
15	C	4-methyl-5H-Furan-2-one	0.91	0.39	0.72	0.76	0.57
16	L	o-Cresol	0.15	0.10	0.22	0.15	0.19
17	L	m-Cresol	0.24	0.31	0.30	0.21	0.37
18	L	Guaiacol	0.85	0.20	0.44	0.72	0.69
19	L	2-ethyl-Phenol	0.42	0.10	0.06	0.25	0.08
20	L	4-methyl Guaiacol	0.69	0.24	0.54	0.57	0.44
21	L	Catechol	1.66	0.84	2.25	1.75	1.88
22	L	3-ethyl-5-methyl-Phenol	0.18	0.19	0.11	0.06	0.13
23	L	3-methyl Catechol	0.68	0.42	0.88	0.70	0.82
24	L	4-ethyl Guaiacol	0.50	0.23	0.21	0.27	0.40
25	L	4-methyl Catechol	0.21	0.10	1.03	0.64	1.00
26	L	4-vinyl Guaiacol	0.95	0.42	0.53	0.70	0.52
27	L	Syringol	0.99	0.47	0.56	0.86	0.98
28	L	Eugenol	0.34	0.49	0.20	0.35	0.27
29	L	3-methoxy Guaiacol	0.37	0.10	0.24	0.40	0.43
30	L	4-ethyl Catechol	0.69	0.34	0.93	0.40	0.76
31	L	Vanillin	0.47	0.18	0.33	0.34	0.29
32	L	4-methyl Syringol	1.39	1.33	0.55	1.50	0.65
33	L	Isoeugenol (trans)	1.20	0.39	0.52	0.90	0.72
34	L	Acetoguaiacone	0.28	0.00	0.17	0.27	0.22
35	C	Levoglucosan	17.68	119.38	44.78	25.62	21.21
36	L	4-vinyl Syringol	2.35	1.49	0.40	1.03	1.47
37	L	*cis*-4-propenyl Syringol	0.50	0.00	0.25	0.51	0.28
38	L	Coniferyl alcohol	1.22	0.00	0.00	0.67	0.62
39	L	*trans*-4-propenyl Syringol	0.37	0.00	0.00	0.28	0.16
40	L	Syringaldehyde	0.97	0.00	0.61	0.81	0.68
41	L	methoxy Eugenol	1.88	0.00	0.68	1.39	0.93
42	L	Acetosyringone	0.60	0.00	0.36	0.51	0.45
43	L	Coniferyl aldehyde	0.48	0.00	0.00	0.33	0.37
44	L	Sinapaldehyde	0.34	0.00	0.17	0.26	0.22
		Total	**99.81**	**182.84**	**109.87**	**101.65**	**108.55**

[a] Carbohydrate derivatives; [b] Lignin derivative

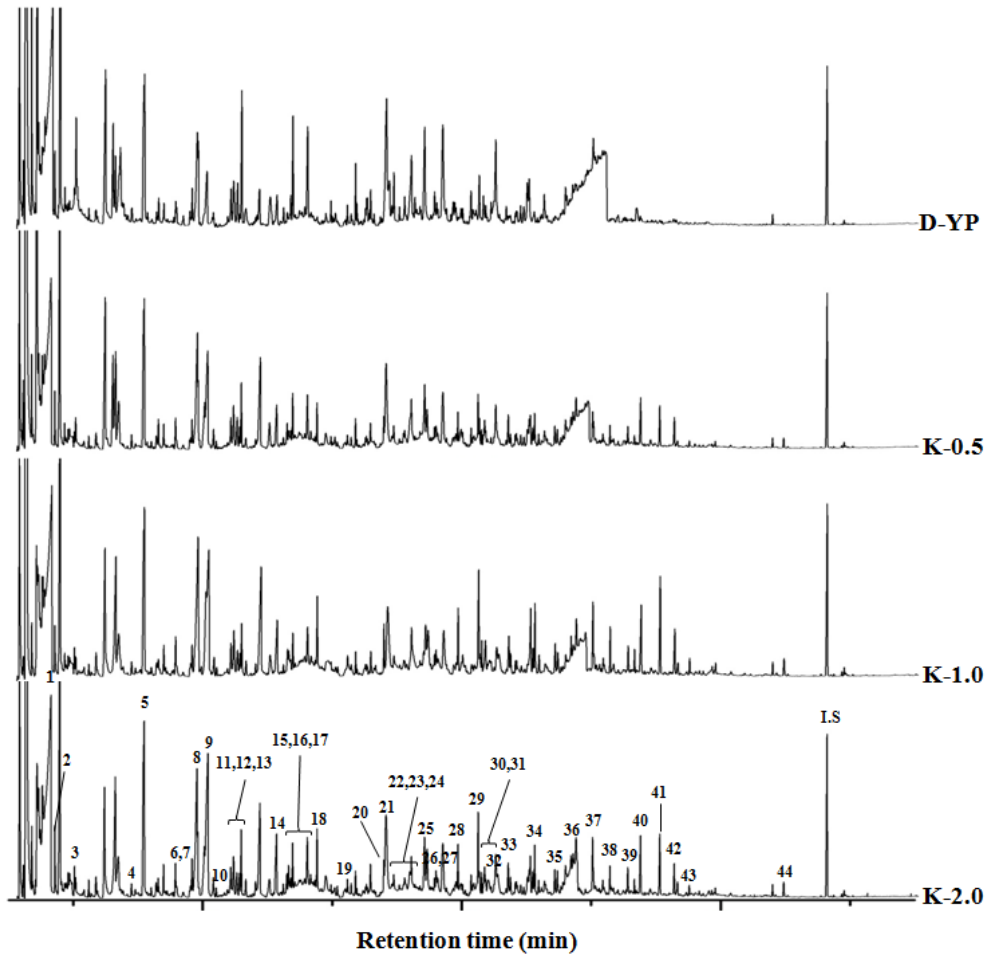

Figure 10 GC-MS chromatogram for bio-oil from potassium-impregnated biomass pyrolyzed at 450°C.

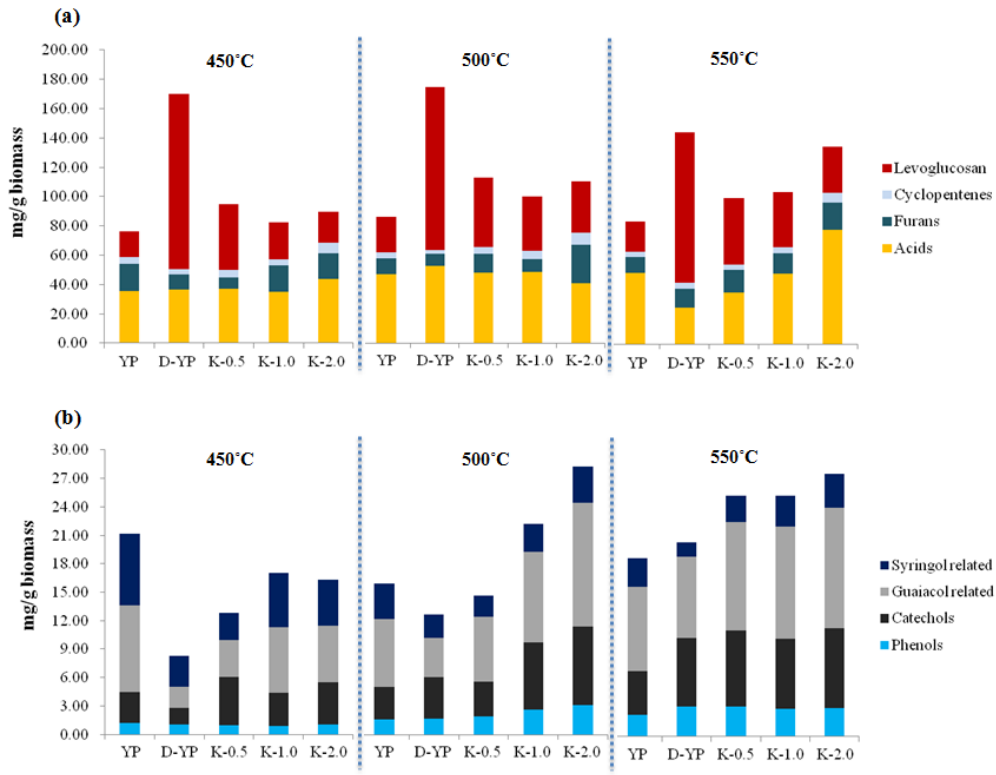

Figure 11 Effect of potassium on the amount of different groups of chemical compounds derived from carbohydrates (a) and lignin (b).

4.5. Effect of magnesium on the characteristics of pyrolytic products

4.5.1. Physicochemical properties of pyrolytic products

The effects of magnesium on the physicochemical properties of pyrolytic products are shown in Table 9 and Figures 12 and 13. As the magnesium content increased, the amount of carbon in the bio-oil slightly decreased while the amount of oxygen increased. This could be a result from of the dehydration reaction promoted by magnesium. Meanwhile the amount of oxygen in bio-oil and bio-char ranged from 44.3% to 46.5% and from 20.0% to 24.4%, respectively. Both amounts of oxygen were higher than that of bio-oil and bio-char from potassium-impregnated samples. These results could be related to the high content of oxygenated compounds in bio-oil including GC-MS-detectable monomers (Table 10) or oligomers. In addition, the high oxygen content of bio-char from magnesium-impregnated samples could be attributed not only to the production of magnesium oxide during pyrolysis, but also to the combination of carbonyl groups on the surface of bio-char and magnesium due to the thermal stability (Wu et al., 2002; Keown et al., 2005; Liu et al., 2013). As the pyrolysis temperature increased, however, the functional groups such as carbonyl groups in bio-char were released by the bond cleavages and the amount of oxygen slightly decreased.

The HHVs of bio-oil and bio-char were estimated to be 18.8–19.5 MJ/kg and 24.1–25.3 MJ/kg, respectively. These values were less than those of the potassium-impregnated samples but there were no significant differences. On the other hand, the pH values of the bio-oil were largely influenced by magnesium. The pH of the bio-oil for Mg-0.5 was similar to other bio-oils, but those of Mg-1.0 and Mg-2.0 were dramatically decreased. Further investigations of these results are ongoing in our laboratory.

Figures 12 and 13 show the water content and viscosity of the bio-oils with different concentrations of magnesium at varying pyrolysis temperatures. As shown in Figure 12, the water content of the bio-oil increased by the dehydration reaction where magnesium acted as a Lewis acid and through the cleavage of the glycosidic bonds of the biomass (Wang et al., 2010). Furthermore the dehydration reaction was accelerated at 550°C. According to the literature, Mg^{2+} has a strong hydration ability and the combination of water and Mg^{2+} is difficult to break down at temperatures higher than the boiling point of water (Bart and Roovers, 1995). Dehydration of the hydrated magnesium ion has been observed even above 500°C, so this could affect the water content of bio-oils produced at different temperatures (Shimada et al., 2007; Shimada et al., 2008).

Magnesium also had an influence on the viscosity of bio-oil (Figure 13). Specifically, the viscosity increased as the magnesium content increased and it was 216 cSt for Mg-2.0 pyrolyzed at 500°C. The viscosity of bio-oil is related to the water content, molecular weight of the constituent compounds, and the presence of submicron char particles in the bio-oil (Bridgwater et al., 1999; Lu et al., 2009). Thus, considering the water content of the bio-oil (Figure 12), the large fractions of the bio-oil produced by magnesium influenced the viscosity. Two supplementary experiments were performed to verify this phenomenon. Tables 10 and 11 show the solid content and the average molecular weight of bio-oils pyrolyzed at 500°C, respectively. Inorganic metals enhanced the formation of char particles. Specifically, a higher solid content was observed with magnesium as compared to potassium. In addition, both the number and weight average molecular weight of the bio-oil for Mg-2.0 were significantly larger than those of the bio-oils for YP, D-YP and K-2.0. These results could be attributed to the recombination reactions induced by magnesium (discussed in Section 4.5.2) along with the chemical composition of the bio-oil.

Table 9 Physicochemical properties of bio-oil and bio-char obtained from magnesium-impregnated biomass.

	Temperature (˚C)								
	450			500			550		
Sample	Mg-0.5	Mg-1.0	Mg-2.0	Mg-0.5	Mg-1.0	Mg-2.0	Mg-0.5	Mg-1.0	Mg-2.0
Bio-oil									
Elemental analysis (%)									
Carbon	46.1	45.6	45.3	45.2	44.1	44.0	46.5	44.3	43.3
Hydrogen	6.4	6.8	6.8	6.6	6.9	7.0	6.8	7.0	7.1
Nitrogen	0.1	0.1	0.1	0.1	0.1	0.1	0.1	0.1	0.1
Oxygen*	47.4	47.5	47.8	48.1	48.9	48.9	46.6	48.6	49.5
HHV(MJ/kg)	19.1	19.2	19.1	19.0	18.9	18.9	19.5	19.0	18.8
pH	2.4	0.6	0.3	2.3	0.6	0.3	2.5	0.7	0.3
Bio-char									
Elemental analysis (%)									
Carbon	75.5	74.7	72.3	76.3	76.6	75.5	77.1	76.3	77.1
Hydrogen	2.4	2.3	2.8	2.3	2.8	2.7	1.4	1.7	2.3
Nitrogen	0.6	0.6	0.5	0.7	0.6	0.6	0.5	0.5	0.5
Oxygen*	21.5	22.4	24.4	20.7	20.0	21.2	21.0	21.5	20.1
HHV(MJ/kg)	24.7	24.4	24.1	24.8	25.3	24.9	24.5	24.4	25.1

*by difference

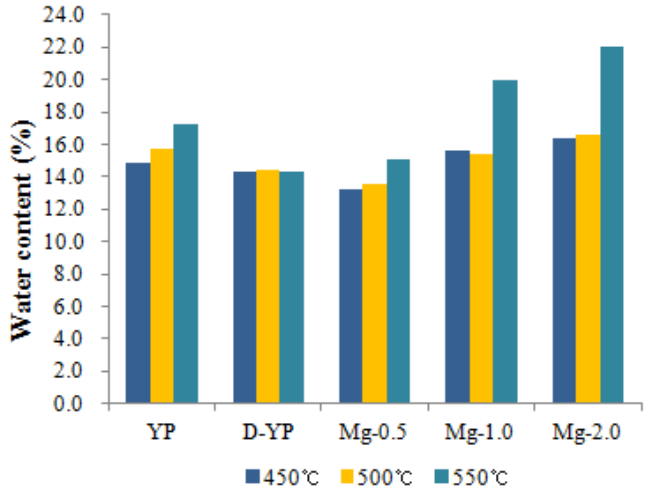

Figure 12 Water content of bio-oil produced under various conditions of magnesium content and pyrolysis temperature.

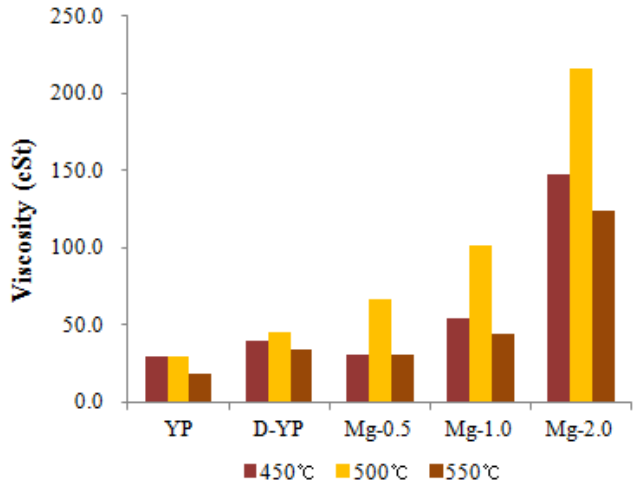

Figure 13 Viscosity of bio-oil produced under various conditions of magnesium content and pyrolysis temperature.

Table 10 Solid content of bio-oil from potassium and magnesium-impregnated biomass (LP : larger particles filtered by 20-25 μm and SP : smaller paricles filtered by 0.50 μm, respectively).

	YP	D-YP	K-2.0	Mg-2.0
LP	0.52	0.05	0.18	0.31
SP	0.29	0.32	0.24	0.42
Total	0.81	0.37	0.42	0.73

Table 11 Average molecular weight of bio-oil from potassium and magnesium-impregnated biomass.

	YP	D-YP	K-2.0	Mg-2.0
Mn	400	483	408	558
Mw	639	946	842	1671
PDI*	1.60	1.96	2.06	2.99

*Polydispersity index

4.5.2. Chemical compounds in bio-oil

The chemical compounds detected by GC-MS analysis are listed in Table 12 and the amount of each group is given in Figure 15. In short, the amount of each chemical group decreased as the magnesium content increased and may be due to the recombination reaction induced by magnesium, as described below.

Inorganic metals in biomass act as a catalyst for the decomposition of glycosidic units by a heterolytic mechanism during pyrolysis (Richards, 1987; Julien et al., 1991). Potassium, as a Lewis acid, could induce the decomposition of the checmical compounds to form small molecules (as mentioned in Section 4.4.2). On the other hand alkaline earth metals have been reported to have conflicting influences and little is known concerning their effect on bio-oil (Varhegyi et al., 1988; Kawamoto et al., 2008). Magnesium would also act as a Lewis acid, but because it is relatively strong Lewis acid it could work differently than potassium. Kawamoto et al. reported that the affinity of Mg^{2+} for the ring oxygen of levoglucosan might result in the ring-opening polymerization of each levoglucosan (Kawamoto et al., 2003a; Kawamoto et al., 2003b). Additionally, the catalytic activities of magnesium on the production of higher molecular weight compounds than levoglucosan were estimated to be about 5.0 while those of potassium were estimated to be about 0.3 (Kawamoto et al., 2008).

Furthermore as magnesium is a divalent ion, it would form two bonds simultaneously, leading to a high concentration of chemicals that may lead to various reactions among the compounds. Therefore, the amount of levoglucosan (Figure 15 (a)) may have been reduced due to the initial decomposition of the biomass or the secondary recombination by magnesium. The reduction range was smaller than that of potassium due to the secondary cracking reaction, and the amount of levoglucosan in bio-oil for Mg-2.0 was 93.35 mg/g, 87.52 mg/g, and 68.53 mg/g with increasing temperatures from 450°C to 550°C.

The amount of lignin groups (Figure 15 (b)) decreased with magnesium that indicated that the lignin polymer was not decomposed by magnesium. With a high content of magnesium, all groups derived from lignin were reduced especially catechols and guaiacol-related groups. This could be due to the formation of large molecules such as oligomers, usually called pyrolytic lignin, and char particles via reactions of the functional sites (Figure 14) rather than gasification (Table 5).

The chemical composition was also affected by temperature. As the temperature increased from 450°C to 550°C, the amount of syringol-related groups decreased from 3.29 mg/g to 2.30 mg/g for D-YP, whereas it decreased from 1.56 mg/g to 0.44 mg/g for Mg-2.0. In addition, the amount of guaiacol-related groups slightly increased from 2.25 mg/g to 2.62 mg/g at 450°C, whereas it decreased from 8.59 mg/g to 1.44 mg/g at 550°C for D-YP and for Mg-2.0, respectively.

Table 12 Comparison of concentration of chemical compounds in bio-oil pyrolyzed from magnesium-impregnated biomass at 450°C.

No.	Source	Compound	Concentration (mg/g biomass)				
			YP	D-YP	Mg-0.5	Mg-1.0	Mg-2.0
1	C[a]	Acetic acid	35.78	36.71	32.23	37.07	38.15
2	C	1-hydroxy-2-Propanone	1.90	2.42	4.94	2.69	0.95
3	C	3-hydroxy-2-Butanone	0.20	1.74	0.12	0.09	0.05
4	C	3-Furaldehyde	0.34	0.49	0.16	0.27	0.11
5	C	Furfural	5.54	4.97	3.88	5.29	3.25
6	C	2-Cyclopentene-1,4-dione	0.60	0.21	0.29	0.23	0.19
7	C	2-metyl-2-Cyclopenten-1-one	0.50	0.65	0.25	0.29	0.23
8	C	2(5H)-Furanone	9.94	2.60	4.37	4.90	3.67
9	C	1,2-Cyclopentanedione	1.81	2.06	1.46	1.64	0.51
10	C	5-metyl-2(5H)-Furanone	0.71	0.51	3.24	3.62	4.23
11	C	5-methyl-2-Furancarboxaldehyde	0.82	0.99	0.87	1.03	0.43
12	C	2H-Pyran-2-one	0.29	0.55	0.81	0.82	0.85
13	L[b]	Phenol	0.21	0.35	0.38	0.39	0.44
14	C	3-methyl-1,2-Cyclopentanedione	1.61	0.86	0.66	0.73	0.73
15	C	4-methyl-5H-Furan-2-one	0.91	0.39	0.65	0.69	0.40
16	L	o-Cresol	0.15	0.10	0.26	0.23	0.34
17	L	m-Cresol	0.24	0.31	0.36	0.28	0.23
18	L	Guaiacol	0.85	0.20	0.00	0.00	0.20
19	L	2-ethyl-Phenol	0.42	0.10	0.06	0.08	0.00
20	L	4-methyl Guaiacol	0.69	0.24	2.13	1.74	1.75
21	L	Catechol	1.66	0.84	0.18	0.30	0.29
22	L	3-ethyl-5-methyl-Phenol	0.18	0.19	0.18	0.16	0.12
23	L	3-methyl Catechol	0.68	0.42	0.65	0.87	0.41
24	L	4-ethyl Guaiacol	0.50	0.23	0.13	0.16	0.13
25	L	4-methyl Catechol	0.21	0.10	0.51	0.51	0.23
26	L	4-vinyl Guaiacol	0.95	0.42	0.16	0.26	0.11
27	L	Syringol	0.99	0.47	0.78	0.64	0.26
28	L	Eugenol	0.34	0.49	0.12	0.06	0.07
29	L	3-methoxy Guaiacol	0.37	0.10	0.11	0.03	0.06
30	L	4-ethyl Catechol	0.69	0.34	1.27	1.00	0.60
31	L	Vanillin	0.47	0.18	0.13	0.10	0.05
32	L	4-methyl Syringol	1.39	1.33	2.47	2.32	1.60
33	L	Isoeugenol (trans)	1.20	0.39	0.25	0.20	0.07
34	L	Acetoguaiacone	0.28	0.00	0.11	0.13	0.07
35	C	Levoglucosan	17.68	119.38	93.35	87.52	68.53
36	L	4-vinyl Syringol	2.35	1.49	0.17	0.37	0.12
37	L	*cis*-4-propenyl Syringol	0.50	0.00	0.26	0.05	0.04
38	L	Coniferyl alcohol	1.22	0.00	0.16	0.14	0.13
39	L	*trans*-4-propenyl Syringol	0.37	0.00	0.06	0.04	0.02
40	L	Syringaldehyde	0.97	0.00	0.33	0.42	0.19
41	L	methoxy Eugenol	1.88	0.00	0.02	0.00	0.00
42	L	Acetosyringone	0.60	0.00	0.01	0.03	0.00
43	L	Coniferyl aldehyde	0.48	0.00	0.00	0.00	0.00
44	L	Sinapaldehyde	0.34	0.00	0.11	0.07	0.08
		Total	**99.81**	**182.84**	**158.64**	**157.46**	**129.89**

[a] Carbohydrate derivatives; [b] Lignin derivatives

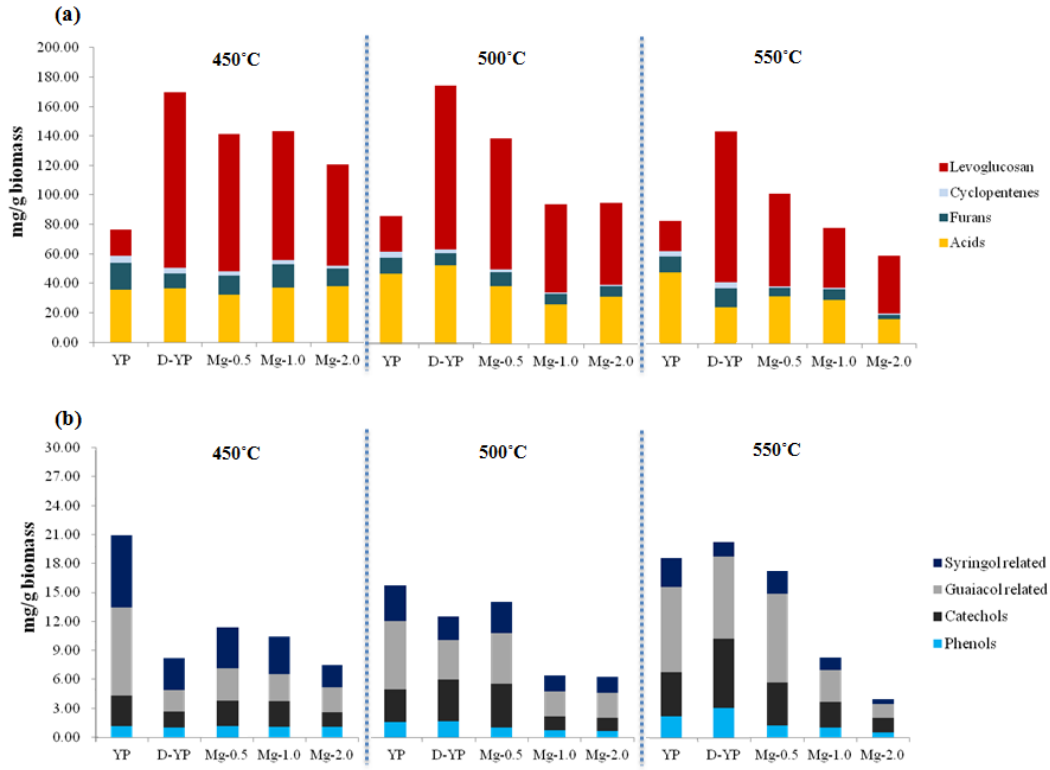

Figure 14 Effect of magnesium on the amount of different groups of chemical compounds derived from carbohydrates (a) and lignin (b).

4.6. Distribution of inorganic metals in pyrolytic products

The inorganic metals in bio-char and bio-oil were analyzed to investigate their distribution and behavior during pyrolysis (Figures 16 and 17). Since most inorganic metals in the biomass were composed of K, Ca, and Mg, their contents were estimated. The amount of bio-char in D-YP samples was too little to allow for analysis by ICP-ES. The potassium and magnesium content of the pyrolytic products gradually increased with impregnated concentration and there was a distinct difference in the residual amounts of bio-oil and bio-char regardless of the type of inorganic metal. The char that contained a high amount of potassium after pyrolysis can be used for burn-out fuel with a high conversion rate, as the combustion is catalyzed by potassium (Jensen et al., 1998; Jones et al., 2004).

Table 13 provides data on the recovery rate of inorganic metals. Approximately 85–94% of inorganic metals remained in the bio-char, in agreement with prior observations (Agblevor and Besler, 1996; Jendoubi et al., 2011). As the temperature increased, however, the total recovery rate gradually decreased and the rate of char decreased while the rate of the oil slightly increased, indicating that the release behavior of inorganic metals is related to pyrolysis temperature. Inorganic metals in biomass likely exist as inorganic salts or in an ionized state combined with oxygen-containing functional groups, although the exact state remains to be clarified (Jensen et al., 2000). As biomass decomposes, inorganic metals are partially released from the biomass and some would be present in the char while others would evaporate after pyrolysis. In addition, inorganic metals in char possibly form intercalation compounds with the surface layer of char (Kapteijn et al., 1983; Sharma et al., 2004). Thus, high temperatures would enhance the decomposition of biomass and the cleavage of weaker bonds between inorganic metals and the char surface. Consequently, this would lead to

a greater release of inorganic metals, so the amount remaining in the char would probably decrease. Moreover, some of the inorganic metals were perhaps caught in the bio-oil and consequently, the recovery rate increased at high temperatures.

Table 13 Recovery rates of inorganic metals from bio-oil and bio-char.

		Recovery rate (%)*		
		450°C	500°C	550°C
Potassium-impregnated biomass	Bio-oil	3.5	4.3	5.5
	Bio-char	93.9	89.6	87.7
	Total	97.4	93.9	93.2
Magnesium-impregnated biomass	Bio-oil	3.9	5.2	5.8
	Bio-char	92.5	89.5	85.1
	Total	96.4	94.7	90.9

* The ratio of inorganic concentrations between pyrolytic products and biomass.

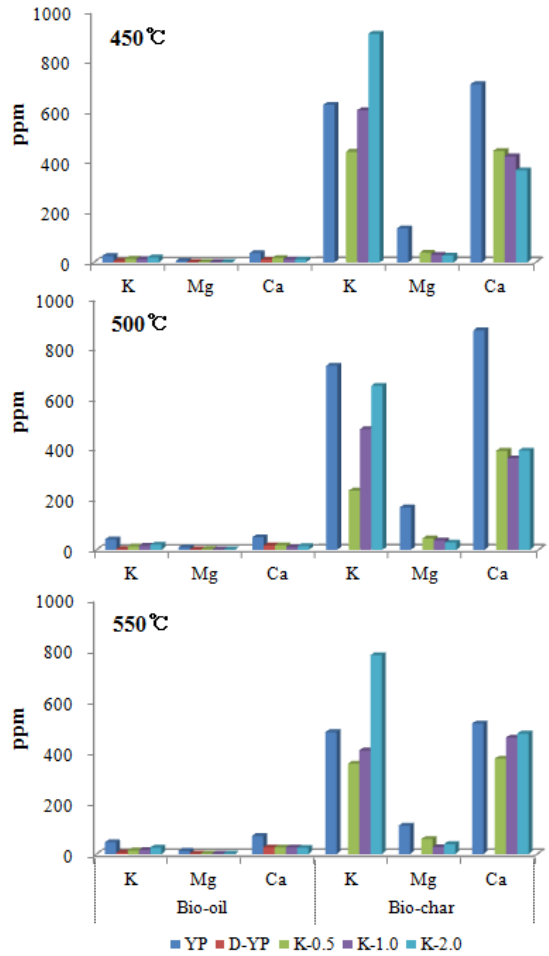

Figure 15 Inorganic distributions in bio-oil and bio-char produced from potassium-impregnated biomass.

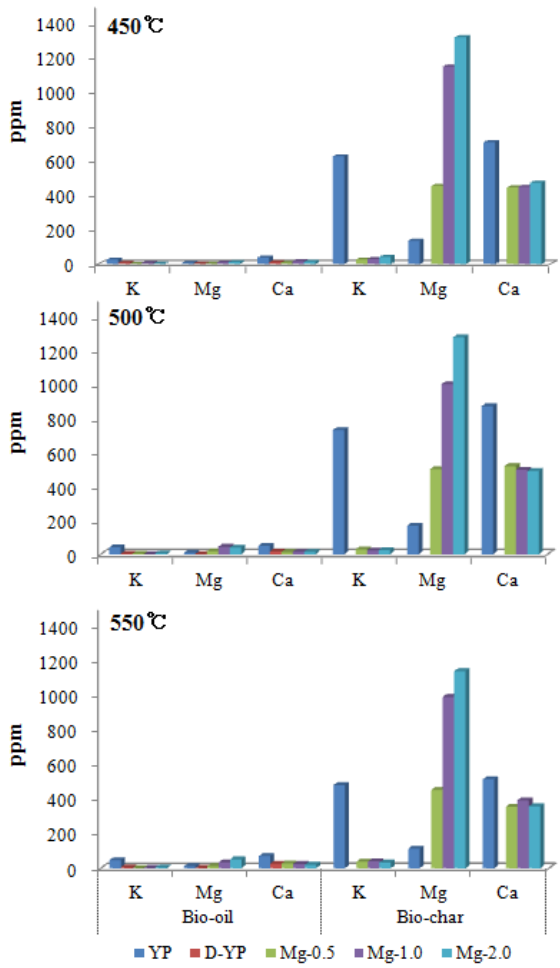

Figure 16 Inorganic distributions in bio-oil and bio-char produced from magnesium-impregnated biomass.

Table 14 Summary of the influences of potassium and magnesium on biomass pyrolysis.

	Influence on				
	Thermal stability	Char formation	Dehydration	Secondary cracking to form smaller fractions in bio-oil	Re-polymerization to form larger fractions in bio-oil
Potassium-impregnated biomass	Medium	Large	Medium	Large	Small
Magnesium-impregnated biomass	Large	Medium	Medium	Small	Large

5. Conclusion

The fast pyrolysis of YP with various concentrations of potassium and magnesium was carried out at different temperatures to investigate the catalytic effects and behaviors of the metals during pyrolysis. TGA revealed that the overall decomposition temperature of the biomass decreased with potassium and magnesium. Char formation was facilitated, whereas the bio-oil yield was not altered significantly. The properties and composition of the bio-oil were largely influenced by the inorganic metals. Specifically, the water content increased due to the dehydration reaction catalyzed by potassium and magnesium, while the chemical composition of the bio-oil differed depending on the type of metal. Small molecules derived from the biomass of the bio-oil increased due to demethoxylation and other secondary reactions promoted by potassium. Magnesium, however, induced the recombination of levoglucosan and small molecules to form large fractions such as oligomers and char particles. Aromatic hydrocarbons were identified in the non-condensed pyrolytic compounds trapped in acetone. The functional groups of the constituent compounds could affect the condensation of the volatiles. Most of the inorganic metals remained in the bio-char and their release during pyrolysis depended on the temperature.

6. References

Agblevor, F., Besler, S.,Evans, R. (1994) Inorganic compounds in Biomass Feedstocks: Their Role in Char Formation and Effect on the Quality of Fast Pyrolysis Oils. proceedings of Biomass Pyrolysis Oil Properties and Combustion Meeting, September, pp. 26-28.

Agblevor, F.,Besler, S. (1996) Inorganic compounds in biomass feedstocks. 1. Effect on the quality of fast pyrolysis oils. Energy & Fuels. 10:293-298.

Bart, J.,Roovers, W. (1995) Magnesium chloride—ethanol adducts. Journal of Materials Science. 30:2809-2820.

Bridgwater, A., Meier, D.,Radlein, D. (1999) An overview of fast pyrolysis of biomass. Org. Geochem. 30:1479-1493.

Bridgewater, A.V. (2004) Biomass fast pyrolysis. Thermal Science. 8:21-50.

Bridgwater, A.V. (2012) Review of fast pyrolysis of biomass and product upgrading. Biomass Bioenergy. 38:68-94.

Chaiwat, W., Hasegawa, I., Kori, J.,Mae, K. (2008) Examination of degree of cross-linking for cellulose precursors pretreated with acid/hot water at low temperature. Ind. Eng. Chem. Res. 47:5948-5956.

Demirbas, A. (2004) Effects of temperature and particle size on bio-char yield from pyrolysis of agricultural residues. J. Anal. Appl. Pyrolysis. 72:243-248.

Elliott, D.C., Oasmaa, A., Preto, F., Meier, D.,Bridgwater, A.V. (2012) Results of the IEA round robin on viscosity and stability of fast pyrolysis bio-oils. Energy & Fuels. 26:3769-3776.

Eom, I.-Y., Kim, K.-H., Kim, J.-Y., Lee, S.-M., Yeo, H.-M., Choi, I.-G.,Choi, J.-W. (2011) Characterization of primary thermal degradation features of lignocellulosic biomass after removal of inorganic metals by diverse solvents. Bioresour Technol. 102:3437-3444.

Eom, I.Y., Kim, J.Y., Kim, T.S., Lee, S.M., Choi, D., Choi, I.G.,Choi, J.W. (2012a) Effect of essential inorganic metals on primary thermal degradation of lignocellulosic biomass. Bioresour Technol. 104:687-694.

Eom, I.Y., Kim, J.Y., Lee, S.M., Cho, T.S., Yeo, H.,Choi, J.W. (2012b) Comparison of pyrolytic products produced from inorganic-rich and demineralized rice straw (Oryza sativa L.) by fluidized bed pyrolyzer for future biorefinery approach. Bioresour Technol.

Fahmi, R., Bridgwater, A., Darvell, L., Jones, J., Yates, N., Thain, S.,Donnison, I. (2007) The effect of alkali metals on combustion and pyrolysis of Lolium and Festuca grasses, switchgrass and willow. Fuel. 86:1560-1569.

Fahmi, R., Bridgwater, A., Donnison, I., Yates, N.,Jones, J. (2008) The effect of lignin and inorganic species in biomass on pyrolysis oil yields, quality and stability. Fuel. 87:1230-1240.

Faix, O., Meier, D.,Fortmann, I. (1990) Thermal degradation products of wood. Holz Roh Werkst. 48:281-285.

Faix, O., Fortmann, I., Bremer, J.,Meier, D. (1991) Thermal degradation products of wood. Holz Roh Werkst. 49:213-219.

Jakab, E., Faix, O., Till, F.,Székely, T. (1993) The effect of cations on the thermal decomposition of lignins. J. Anal. Appl. Pyrolysis. 25:185-194.

Jendoubi, N., Broust, F., Commandre, J., Mauviel, G., Sardin, M.,Lédé, J. (2011) Inorganics distribution in bio oils and char produced by biomass fast pyrolysis: The key role of aerosols. J. Anal. Appl. Pyrolysis. 92:59-67.

Jensen, A., Dam-Johansen, K., Wójtowicz, M.A.,Serio, M.A. (1998) TG-FTIR study of the influence of potassium chloride on wheat straw pyrolysis. Energy & Fuels. 12:929-938.

Jensen, P.A., Frandsen, F., Dam-Johansen, K.,Sander, B. (2000) Experimental investigation of the transformation and release to gas phase of potassium and chlorine during straw pyrolysis. Energy & Fuels. 14:1280-1285.

Jones, J., Williams, A., Darvell, L., Nawaz, M.,Baxter, X. (2004) The role of metals in biomass pyrolysis, char formation and char properties. Science in Thermal and Chemical Biomass Conversion, Victoria, Canada. 30:1203-1214.

Julien, S., Chornet, E., Tiwari, P.,Overend, R. (1991) Vacuum pyrolysis of cellulose: Fourier transform infrared characterization of solid residues, product distribution and correlations. J. Anal. Appl. Pyrolysis. 19:81-104.

Kapteijn, F., Jurriaans, J.,Moulijn, J.A. (1983) Formation of intercalate-like structures by heat treatment of K_2CO_3-carbon in an inert atmosphere. Fuel. 62:249-251.

Kawamoto, H., Hatanaka, W.,Saka, S. (2003a) Thermochemical conversion of cellulose in polar solvent (sulfolane) into levoglucosan and other low molecular-weight substances. J. Anal. Appl. Pyrolysis. 70:303-313.

Kawamoto, H., Murayama, M.,Saka, S. (2003b) Pyrolysis behavior of levoglucosan as an intermediate in cellulose pyrolysis: polymerization into polysaccharide as a key reaction to carbonized product formation. Journal of Wood Science. 49:469-473.

Kawamoto, H., Yamamoto, D.,Saka, S. (2008) Influence of neutral inorganic chlorides on primary and secondary char formation from cellulose. Journal of Wood Science. 54:242-246.

Keown, D.M., Favas, G., Hayashi, J.-i.,Li, C.-Z. (2005) Volatilisation of alkali and alkaline earth metallic species during the pyrolysis of biomass: differences between sugar cane bagasse and cane trash. Bioresour. Technol. 96:1570-1577.

Kim, K.H., Eom, I.Y., Lee, S.M., Choi, D., Yeo, H., Choi, I.G.,Choi, J.W. (2011) Investigation of physicochemical properties of biooils produced from yellow poplar wood (Liriodendron tulipifera) at various temperatures and residence times. J. Anal. Appl. Pyrolysis. 92:2-9.

Kowalski, T.L., C.,Wokaun, A. (2007) Qualitative evaluation of alkali release during the pyrolysis of biomass. Energy & Fuels. 21:3017-3022.

Liu, W.-J., Jiang, H., Tian, K., Ding, Y.-W.,Yu, H.-Q. (2013) Mesoporous Carbon Stabilized MgO Nanoparticles Synthesized by Pyrolysis of $MgCl_2$ Preloaded Waste Biomass for Highly Efficient CO_2 Capture. Environmental science & technology. 47:9397-9403.

Lu, Q., Li, W.Z.,Zhu, X.F. (2009) Overview of fuel properties of biomass fast pyrolysis oils. Energy Convers. Manage. 50:1376-1383.

Milne, T., Agblevor, F., Davis, M., Deutch, S.,Johnson, D. (1997) A review of the chemical composition of fast pyrolysis oils from biomass. Developments in Thermalchemical Biomass Conversion. 1:409-424.

Mohan, D., Pittman Jr, C.U.,Steele, P.H. (2006) Pyrolysis of wood/biomass for bio-oil: a critical review. Energy & Fuels. 20:848-889.

Morishita, T., Tsumura, T., Toyoda, M., Przepiórski, J., Morawski, A., Konno, H.,Inagaki, M. (2010) A review of the control of pore structure in MgO-templated nanoporous carbons. Carbon. 48:2690-2707.

Moses, C.A.,Bernstein, H. (1994) Impact study on the use of biomass-derived fuels in gas turbines for power generation. National Renewable Energy Lab., Golden, CO (United States); Southwest Research Inst., San Antonio, TX (United States).

Mourant, D., Wang, Z., He, M., Wang, X.S., Garcia-Perez, M., Ling, K.,Li, C.-Z. (2011) Mallee wood fast pyrolysis: Effects of alkali and alkaline earth metallic species on the yield and composition of bio-oil. Fuel. 90:2915-2922.

Nimlos, M.R., Blanksby, S.J., Ellison, G.B.,Evans, R.J. (2003) Enhancement of 1, 2-dehydration of alcohols by alkali cations and protons: a model for dehydration of carbohydrates. J. Anal. Appl. Pyrolysis. 66:3-27.

Nowakowski, D., Jones, J., Brydson, R.,Ross, A. (2007) Potassium catalysis in the pyrolysis behaviour of short rotation willow coppice. Fuel. 86:2389-2402.

Nowakowski, D.J.,Jones, J.M. (2008) Uncatalysed and potassium-catalysed pyrolysis of the cell-wall constituents of biomass and their model compounds. J. Anal. Appl. Pyrolysis. 83:12-25.

Oasmaa, A.,Peacocke, C. (2001) a guide to physical property characterisation of biomass-derived fast pyrolysis liquids. Technical Research Centre of Finland, VTT Publications. 450.

Onay, O. (2007) Influence of pyrolysis temperature and heating rate on the production of bio-oil and char from safflower seed by pyrolysis, using a well-swept fixed-bed reactor. Fuel Process. Technol. 88:523-531.

Patwardhan, P.R., Satrio, J.A., Brown, R.C.,Shanks, B.H. (2010) Influence of inorganic salts on the primary pyrolysis products of cellulose. Bioresour Technol. 101:4646-4655.

Pittman Jr, C.U., Mohan, D., Eseyin, A., Li, Q., Ingram, L., Hassan, E.B.M., Mitchell, B., Guo, H.,Steele, P.H. (2012) Characterization of Bio-oils Produced from Fast Pyrolysis of Corn Stalks in an Auger Reactor. Energy & Fuels. 26:3816-3825.

Richards, G.N. (1987) Glycolaldehyde from pyrolysis of cellulose. J. Anal. Appl. Pyrolysis. 10:251-255.

Sharma, R.K., Wooten, J.B., Baliga, V.L., Lin, X., Geoffrey Chan, W.,Hajaligol, M.R. (2004) Characterization of chars from pyrolysis of lignin. Fuel. 83:1469-1482.

Sheng, C.,Azevedo, J. (2005) Estimating the higher heating value of biomass fuels from basic analysis data. Biomass Bioenergy. 28:499-507.

Shimada, N., Kawamoto, H.,Saka, S. (2007) Solid-state hydrolysis of cellulose and methyl α-and β-D-glucopyranosides in presence of magnesium chloride. Carbohydrate research. 342:1373-1377.

Shimada, N., Kawamoto, H.,Saka, S. (2008) Different action of alkali/alkaline earth metal chlorides on cellulose pyrolysis. J. Anal. Appl. Pyrolysis. 81:80-87.

Skrifvars, B.-J., Backman, R.,Hupa, M. (1998) Characterization of the sintering tendency of ten biomass ashes in FBC conditions by a laboratory test and by phase equilibrium calculations. Fuel Process. Technol. 56:55-67.

Sluiter, A., Hames, B., Ruiz, R., Scarlata, C., Sluiter, J., Templeton, D.,Crocker, D. (2004) Determination of structural carbohydrates and lignin in biomass. NREL, Golden, CO.

Sluiter, A., Hames, B., Ruiz, R., Scarlata, C., Sluiter, J.,Templeton, D. (2005) Determination of ash in biomass. NREL BAT Team Laboratory Analytical Procedure.

Tsubouchi, N., Xu, C.,Ohtsuka, Y. (2003) Carbon crystallization during high-temperature pyrolysis of coals and the enhancement by calcium. Energy & Fuels. 17:1119-1125.

Varhegyi, G., Antal Jr, M.J., Szekely, T., Till, F.,Jakab, E. (1988) Simultaneous thermogravimetric-mass spectrometric studies of the thermal decomposition of biopolymers. 1. Avicel cellulose in the presence and absence of catalysts. Energy & Fuels. 2:267-272.

Vispute, T.P., Zhang, H., Sanna, A., Xiao, R.,Huber, G.W. (2010) Renewable chemical commodity feedstocks from integrated catalytic processing of pyrolysis oils. Science. 330:1222-1227.

Wang, H., Srinivasan, R., Yu, F., Steele, P., Li, Q., Mitchell, B.,Samala, A. (2012) Effect of Acid, Steam Explosion, and Size Reduction Pretreatments on Bio-oil Production from Sweetgum, Switchgrass, and Corn Stover. Appl Biochem Biotechnol. 167:285-297.

Wang, Z., Wang, F., Cao, J.,Wang, J. (2010) Pyrolysis of pine wood in a slowly heating fixed-bed reactor: Potassium carbonate versus calcium hydroxide as a catalyst. Fuel Process. Technol. 91:942-950.

Wu, H., Quyn, D.M.,Li, C.-Z. (2002) Volatilisation and catalytic effects of alkali and alkaline earth metallic species during the pyrolysis and gasification of Victorian brown coal. Part III. The importance of the interactions between volatiles and char at high temperature. Fuel. 81:1033-1039.

초 록

본 연구에서는 목질계 바이오매스 내 주요 무기 성분인 칼륨과 마그네슘이 바이오매스의 급속 열분해 공정 및 열분해 산물의 특성에 미치는 영향을 구명하고자 하였다. 대표적 속성수인 백합나무를 대상으로 하여 무기성분의 함량을 낮춘 시료와 칼륨과 마그네슘을 농도 별로 침지한 시료를 제조하였으며 각각 열중량 분석과 더불어 급속 열분해 공정을 수행하였다. 이 때 급속 열분해 공정은 450, 500, 550℃ 온도 조건하에 진행되었으며 체류 시간은 1.3초로 고정하였다. 이 후 생산된 바이오오일의 물성을 분석하였다.

열중량 분석 결과 바이오매스에 있는 무기성분의 함량이 높아짐에 따라 바이오매스의 최대 분해 온도가 감소하였으며 이러한 변화는 칼륨에 비해 마그네슘의 영향이 더 큰 것을 확인하였다. 급속 열분해 공정에서는 두 무기성분 모두 탄의 수율을 증가시켰으며 특히 칼륨의 경우 모든 온도 조건에서 무기성분의 함량이 가장 낮은 시료 대비 약 두 배 가량 탄 수율이 증가하였다. 이러한 무기성분들은 바이오오일의 물리·화학적 특성에도 큰 영향을 미쳤으며 칼륨의 농도가 증가함에 따라 오일의 수분 함량은 14.4 wt%에서 19.7 wt%까지 증가하였고 점도는 34 cSt 에서 16 cSt 으로 감소한 반면 산성도는 큰 변화를 나타내지 않았다. 마그네슘의 경우에도 농도가 증가함에 따라 탈수 반응이 촉진되어 수분 함량이 증가하였으나 칼륨과는 달리 점도는 45 cSt 에서 216 cSt 으로 크게 증가하였으며 산성도는 감소하였다. GC-MS 분석 결과 칼륨은 오일 내 levoglucosan 등 화합물을 분해함과 동시에 저분자량의 화합물 및 리그닌 유래 페놀성 화합물을 증가시키는 열화학적 반응을 촉진하는 경향을 보였다. 반면

마그네슘은 levoglucosan 및 기타 저분자량의 화합물 간 재결합 반응의 촉매로 작용하여 저중합체 및 미세 입자 등 상대적으로 큰 화합물의 형성을 유도하는 것으로 나타났다. 열분해 공정 종료 후 대부분의 무기성분은 탄에 존재하였고 이러한 잔류량은 열분해 온도 조건과 관련이 있음을 확인하였다. 또한 리그닌으로부터 유래한 것으로 판단되는 5 종의 방향족 탄화수소를 아세톤 여과장치를 통해 비응축 가스로부터 검출하였다.